

Original Article

Cite this article: Satolli S, Agostini S, and Calamita F (2019) Behaviour of minor arcuate shapes hosted in curved fold-and-thrust belts: an example from the Northern Apennines (Italy). *Geological Magazine* **156**: 1547–1564. <https://doi.org/10.1017/S0016756818000845>

Received: 5 July 2018

Revised: 12 November 2018

Accepted: 14 November 2018

First published online: 28 January 2019

Keywords:

inversion tectonics; palaeomagnetism; structural geology; vertical axis rotations

Author for correspondence: Sara Satolli,
Email: sara.satolli@unich.it

Behaviour of minor arcuate shapes hosted in curved fold-and-thrust belts: an example from the Northern Apennines (Italy)

Sara Satolli^{1,2} , Simone Agostini³ and Fernando Calamita¹ 

¹Dipartimento di Ingegneria e Geologia, Università “G. d’Annunzio” di Chieti-Pescara, 66100 Chieti Scalo, Italy;

²CiMaN-LP – Alpine Laboratory of Paleomagnetism, Via Luigi Massa 4, 12016, Peveragno (CN), Italy and ³CGG Robertson – Tyn-y-Coed, Pentwyn Road, Llandudno, Gwynedd, UK

Abstract

Arcuate fold-and-thrust belts have been extensively studied in the literature. Less attention, however, has been paid to the characteristics of local-scale arcuate structures, meaning 5–10 km long fold or thrust traces that display map-view curvature. Nevertheless, detailed investigation of small arcuate structures hosted in major arcs can contribute to understanding the pervasiveness of deformation mechanisms. We performed a combined geological and palaeomagnetic study on 21 sites from a c. 60 km² area in the Northern Apennines in order to analyse minor arcs at a kilometric scale. As evidenced by the geological and structural analysis performed on the 21 sites, the fold axial trend changes from N–S to NW–SE in the study area. The comparison with palaeomagnetic results shows the lack of correlation between vertical axis rotations and fold axial trends. As a consequence, the minor arcuate shapes of thrusts and related folds are interpreted as mostly primary features inherited from the geometry of the palaeomargin, represented by pre-orogenic faults, according to a context of inversion tectonics.

1. Introduction

There are many examples of arcuate fold-and-thrust belts worldwide that have been extensively studied in the literature. Some examples include the Appalachian (e.g. Bayona *et al.* 2003), Taiwan (e.g. Lacombe *et al.* 2003), the Sevier (e.g. Weil *et al.* 2010), Jura Mountains (Hindle & Burkhard, 1999), Zagros (Aubourg *et al.* 2004), the Western Alps (e.g. Lickorish *et al.* 2002) and the Variscan (Lacquement *et al.* 2005).

Curved orogens are identified depending upon their kinematics as: (1) primary (or non-rotational) arcs, which acquire their curvature without appreciable rotation (Carey, 1955; Marshak, 1988, 2004); (2) secondary (or oroclines or rotational arcs), which are originally linear and are bent during a successive deformation event; and (3) progressive arcs, which develop their arcuate nature as they grow (Weil & Sussman, 2004).

The plan-view curved structural trends of orogenic belts may occur at different scales. It is often possible to recognize smaller arcuate structures inside larger-scale arcuate belts. The attention paid to these smaller curved structures has been limited (e.g. Smith *et al.* 2005; Pastor-Galán *et al.* 2012; Rodríguez-Pintó *et al.* 2016). However, the detailed investigation of individual structures is potentially useful in order to understand what geological factors act on second-order curves hosted on in regional-scale curves.

The presence at different scales of arcuate structures is documented, for instance, in the Apennine–Maghrebide orogeny. Here, the first-order arc (Fig. 1a) is a hundred-kilometric-scale salient with convexity toward the Adria/Africa foreland, characterized by the Calabrian units in the apical zone and the Tyrrhenian extensional basin in the inner area (Johnston & Mazzoli, 2009). The Apennine segment can be further divided into two second-order arcs, characterized by counterclockwise (CCW) and clockwise (CW) rotations in their northern and southern sector, respectively: the Northern Apennines arc with NE convexity and the Southern Apennines – Calabrian arc with SE convexity. These two arcs are also characterized by several differences in palaeogeographic domains, stratigraphic successions, structural setting and geodynamic evolution, with respect to each other (e.g. Malinverno & Ryan, 1986; Carmignani & Kligfield, 1990; Doglioni, 1991; Boccaletti *et al.* 2005; Finetti, 2005; Satolli & Calamita, 2008, 2012). Both these second-order arcs show minor kilometric-scale curved structures, characterized by changes in structural strike (e.g. the Gran Sasso range and the Matese–Frosolone Mountains: Satolli *et al.* 2005; Satolli & Calamita, 2008, 2012).

The first- and second-order arcs of the Apennines have been largely palaeomagnetically investigated over the last 40 years and show widespread differential vertical axes rotations that have been explained with different models. Palaeomagnetic data from back-arc extensional basins along the Tyrrhenian margin show no rotation (e.g. Mattei *et al.* 1996), indicating that the opening of the Tyrrhenian Sea was non-rotational. Conversely, data collected in Mesozoic

and Miocene – Lower Pliocene sediments show varying amounts of rotation, due to both thrusts and strike-slip fault activity. In the Northern Apennines, a change in palaeomagnetic rotations from CCW to CW has been documented moving southward: strong CCW rotations have been documented in the Emilia–Romagna region (Speranza *et al.* 1997; Muttoni *et al.* 1998), while the Sibillini thrust front is characterized by CW rotation in the central sector (Speranza *et al.* 1997). Large CCW and CW rotations are also documented in the Southern Apennines (Scheepers & Langereis, 1994; Speranza *et al.* 1998; Gattacceca & Speranza, 2002) and Sicily (Channell *et al.* 1990; Speranza *et al.* 2003), respectively. Studies from arcs of 10–100 km of amplitude have documented different behaviours: there are minor arcs characterized by CCW and CW rotations along the limbs (Gran Sasso Range (Satolli *et al.* 2005)), block rotations due to strike-slip faults (e.g. Central Apennines (Mattei *et al.* 1995) and Olevano–Antrodoco sibilini thrust (Turtù *et al.* 2013)) and small homogeneous CW-rotated structures (e.g. Mount Maiella (Jackson, 1990) and Mount Greco – Mount Genzana (Marton & D'Andrea, 1992)).

Several decades of research showed that the use of single datasets (e.g. structural data, palaeomagnetism, anisotropy of magnetic susceptibility, seismic reflection and so on) to classify curved features leads to contradictory and incomplete interpretations of their kinematic evolution. That was the case of the Northern Apennines second-order arc, which has been interpreted in the literature either as an orocline (Speranza *et al.* 1997), a primary (Channell *et al.* 1978; Eldredge *et al.* 1985; Muttoni *et al.* 1998) or a progressive arc (Calamita & Deiana, 1988). Recently, the progressive arc kinematic model has been supported by the integration of palaeomagnetic and structural data (Cifelli & Mattei, 2010; Cifelli *et al.* 2016). The development of the first-order arc is attributed to different lithospheric-scale phenomena, including subducting lithosphere rollback (Doglioni, 1991; Lucente & Speranza, 2001; Faccenna *et al.* 2004), gravitational collapse (Carmignani & Kligfield, 1990), orogen-perpendicular compression (Jolivet *et al.* 1990) and orogen-parallel compression (Faccenna *et al.* 1996; Johnston & Mazzoli, 2009). However, minor arcs are controlled by processes occurring at crustal levels that may depend on different factors (e.g. Davis *et al.* 1983; Marshak, 1988, 2004; Marshak *et al.* 1992; Macedo & Marshak, 1999). The main deformation mechanism acting in the Northern Apennines is ascribed to growth of a mid-crustal anticlinorium that acts as an obstacle in an out-of-sequence context (Billi & Tiberti, 2009), or to the influence of inversion tectonics, compatible with a thick-skinned setting of the belt in an in-sequence context (Satolli & Calamita, 2012). Several authors investigated the role of pre-thrusting normal faults in the Apennines belt evolution. Such faults are documented at different scales and were either truncated by thrusts with a short-cut trajectory or reactivated with reverse kinematics, depending upon the trend of pre-existing extensional faults with respect to the subsequent compressional stress field (e.g. Tavarnelli *et al.* 2004; Calamita *et al.* 2012; Di Domenica *et al.* 2012; Scisciani *et al.* 2014).

In particular, the development of the Northern Apennines progressive arc was influenced by the architecture of the Adria palaeomargin (Calamita *et al.* 2012). The system has a component of primary and progressive arc development: its primary curvature was accentuated during orogenesis by CCW and CW tectonic rotations in its northern and southern limbs, respectively (Satolli & Calamita, 2012; Turtù *et al.* 2013). The importance of inversion tectonics has also been shown through palaeomagnetism in minor arcs, as in the case of the Gran Sasso range (central Apennines),

where the Adria palaeomargin played the role of an indenter causing strong rotations in its apex (Satolli *et al.* 2005).

The integrated analysis of geological, structural and palaeomagnetic data has been shown to be a powerful instrument in unravelling the kinematics of curved belts (e.g. Kwon & Mitra, 2004; Weil & Sussman, 2004; Weil *et al.* 2010; Pueyo *et al.* 2016). The aim of this study is to integrate structural and palaeomagnetic data in order to analyse minor arcuate structures in the framework of the Northern Apennines second-order arc, within the larger context of the Apennine–Maghrebide belt.

Minor strongly arcuate structures (e.g. Cingoli, Subasio, Mount Corneto – Mount Prefoglio; Fig. 1b) can be recognized in the Northern Apennines and are potentially good candidates for this study. However, it is crucial to select as far as possible from major strike-slip faults and oblique thrust ramps, which can strongly affect the vertical axis rotations (e.g. Mattei *et al.* 1995; Pueyo *et al.* 2003; Turtù *et al.* 2013). For this reason, we selected the Mount Corneto – Mount Prefoglio anticline and Mount Cesino syncline, a minor arcuate structure located in the inner part of the Northern Apennines and showing N–S and NW–SE axial trend (Fig. 1b; Fig. 3 below).

2. Geological setting

The stratigraphic succession of the Northern Apennines (Fig. 1c) is almost entirely composed of a pre-orogenic Triassic to Miocene carbonate sequence deposited on the continental passive margin of Adria. The Jurassic–Cretaceous pelagic succession exhibits facies and thickness variations controlled by Jurassic syn-sedimentary normal faults (e.g. Santantonio, 1993). The Mesozoic morphology was smoothed during the upper Tithonian–Barremian interval with sedimentation of the Maiolica Formation, followed in the Aptian–Albian interval by the deposition of a continuous marly deposit (Marne a Fucoidi Formation). The stratigraphic succession continues upwards with basinal and hemipelagic cherty limestones (Scaglia Bianca and Scaglia Rossa formations) with intercalations of clayey marls that became prevalent in the Oligocene and Miocene intervals (i.e. Scaglia Cinerea, Bisciaro and Schlier formations). Foredeep siliciclastic deposits unconformably overlie the aforementioned succession showing a progressively younger age from W to E, coherent with a westward propagation of the chain–foredeep system (Boccaletti *et al.* 1990). Quaternary continental deposits unconformably lie above the older units and show maximum thickness in intramontane basins bordered by normal faults, such as in the Colfiorito basin (Fig. 1b).

Minor fold-and-thrust arcuate structures in the Northern Apennines show arcuate trend similar to the Olevano–Antrodoco–Sibillini outer thrust, with the highest amount of shortening corresponding with the apical point (Calamita & Pierantoni, 1993). The shortening achieved by each structure rarely exceeds 2 km. Minor folds due to the competence contrast within the multilayered sedimentary succession (Barchi, 2010) have been widely documented in the Northern Apennines. The orientation of individual thrusts and folds ranges between NW–SE in frontal ramps and N–S in lateral ramps (Calamita *et al.* 2012; Pace & Calamita, 2014, 2015) and is generally representative of the structural trend of the hosting structure. Therefore, these structural elements have been widely studied in order to reconstruct the evolution of the external sector of the Northern Apennines, leading to both buckling (Lavecchia, 1985; Cipollari & Cosentino, 1995) and fault-propagation-fold (Calamita, 1990; Tavarnelli, 1993) genesis

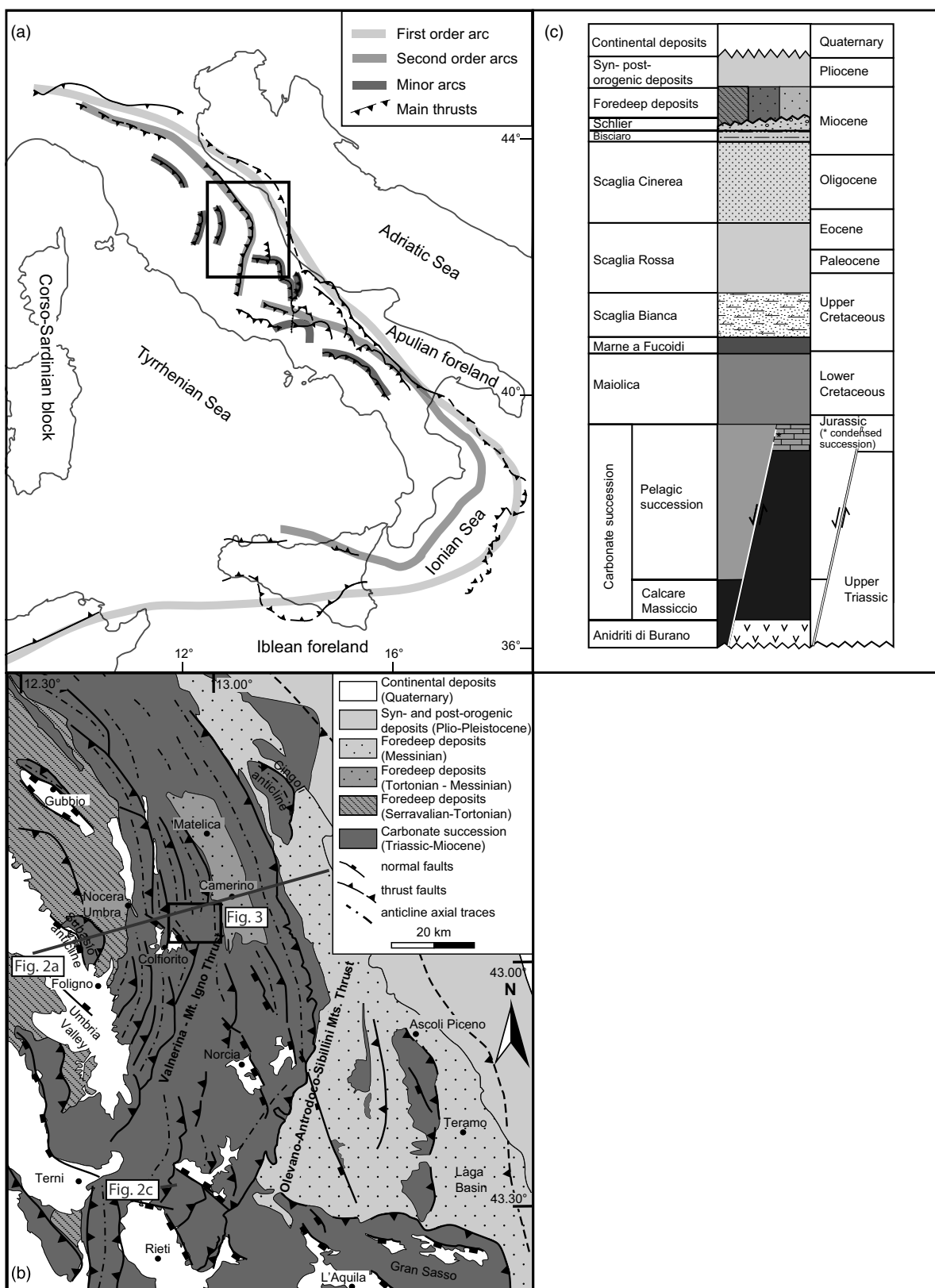


Fig. 1. (a) Tectonic sketch map showing the first-order Apennine–Maghrebide Arc, the Northern Apennines and the Southern Apennines – Calabrian second-order arcs and some minor arcs of the orogenic system; the inset box indicates (b). (b) Schematic geological map of the Central–Northern Apennines showing major thrusts and normal faults; grey lines indicate the location of sections in Figure 2. The inset box indicates the geological map in Figure 3. (c) Schematic stratigraphic succession of the Northern Apennines.

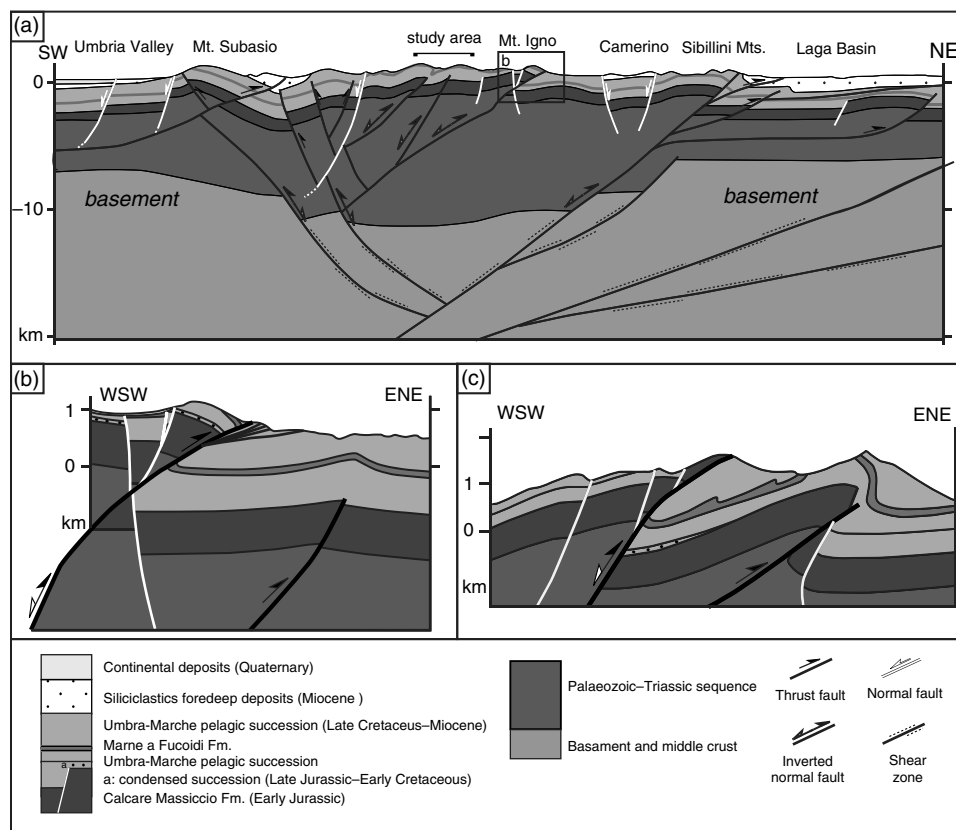


Fig. 2. Examples of positive inversion tectonics in the Northern Apennines at different scales: (a) Crustal geological cross-section showing the involvement of the basement (modified after Scisciani *et al.* 2014); the bracket shows the cross-section in the study area characterized by the blind thrusts and folds (Mount Corneto – Mount Prefoglio anticline and Mount Cesino syncline), related to the positive inversion of pre-thrusting normal faults as documented in the Mount Igno (b) and Mount Coscerno (d) structures. (b) Geological cross-section showing the relationships between the Jurassic normal faults and the Neogene compressional thrust–fold structures in Mount Igno (modified after Scisciani *et al.* 2014). (c) Geological cross-section showing the relationships between the inherited normal faults (Jurassic and/or Miocene) and the Neogene compressional thrust–fold structures in a typical N–S-trending Mount Coscerno structure (located in Fig. 1; modified after Pace *et al.* 2017).

mechanisms. Recently, along-strike variations of the folding mechanisms have been ascribed to the selective control of positive inversion tectonics: NNE–SSW-trending anticlines are reactivated as fault-bend folds, with NW–SE-trending anticlines as fault-propagation folds (Calamita *et al.* 2012; Pace & Calamita, 2015). However, local axial trend variations are observed in some structures, regardless of their position in the hosting arc.

Both thin- and thick-skinned structural styles have been reported for the Apennines either with a simple transition from thick- to thin-skinned tectonics from the inner chain towards the foreland (Bally *et al.* 1986) or with thrust faults affecting the basement in the outer zones of the fold-and-thrust belt (Barchi *et al.* 1998; Finetti, 2005; Scisciani & Montefalcone, 2006). In recent years, a positive inversion of Adria palaeomargin structures has been proposed, suggesting that numerous thrusts are roots in inherited pre-orogenic structures, including Miocene foredeep normal faults (Tavarnelli *et al.* 2004). Moreover, several studies have emphasized the role exerted by the positive reactivation of pre- and syn-orogenic normal faults in the outer sector of the Northern Apennines fold-and-thrust belt (Coward *et al.*, 1999; Scisciani *et al.* 2002; Tozer *et al.* 2002; Tavarnelli *et al.* 2004; Calamita *et al.* 2011; Di Domenica *et al.* 2012; Turtù *et al.* 2013). Recently, Scisciani *et al.* (2014) suggested the coexistence of a positive basement inversion (either with a detaching level within the Triassic succession or with a homogeneous basement-cover deformation where both normal faults and thrusts that

involve the basement cut upwards through the sedimentary cover) to explain the regional arcuate-shaped anticlinorium. According to the balanced crustal geological cross-section (Scisciani *et al.* 2014; Fig. 2a), the blind thrusts related to the N–S-trending sector of the Mount Corneto – Mount Prefoglio anticline and Mount Cesino syncline analysed in this paper can be interpreted as the reactivation of a Jurassic normal fault, in agreement with the interpretation proposed by Scisciani *et al.* 2014 for the Mount Igno structure (Fig. 2b) or for other N–S trending-structures from the Northern Apennines (e.g. the Mount Coscerno structure (Pace *et al.* 2017; Fig. 2c)).

3. Structural and palaeomagnetic analysis

We studied a c. 60 km² area representing one of the inner arcs of the Northern Apennines (Figs 1b and 3), namely the Mount Corneto – Mount Prefoglio anticline and Mount Cesino syncline. This minor arcuate structure shows N–S axial trend in its northern and southern sectors and NW–SE trend in its central one.

The study area is characterized by a series of NE- to E-verging folds with gentle backlimbs and vertical to slightly overturned forelimbs (Calamita & Pierantoni, 1993; Calamita *et al.* 1997). In the western sector, the Mount Corneto – Mount Prefoglio anticline and Mount Cesino syncline are characterized by N–S and NW–SE axial trends, whereas folds and related thrusts show NW–SE and N–S trends in the inner and external sector, respectively.

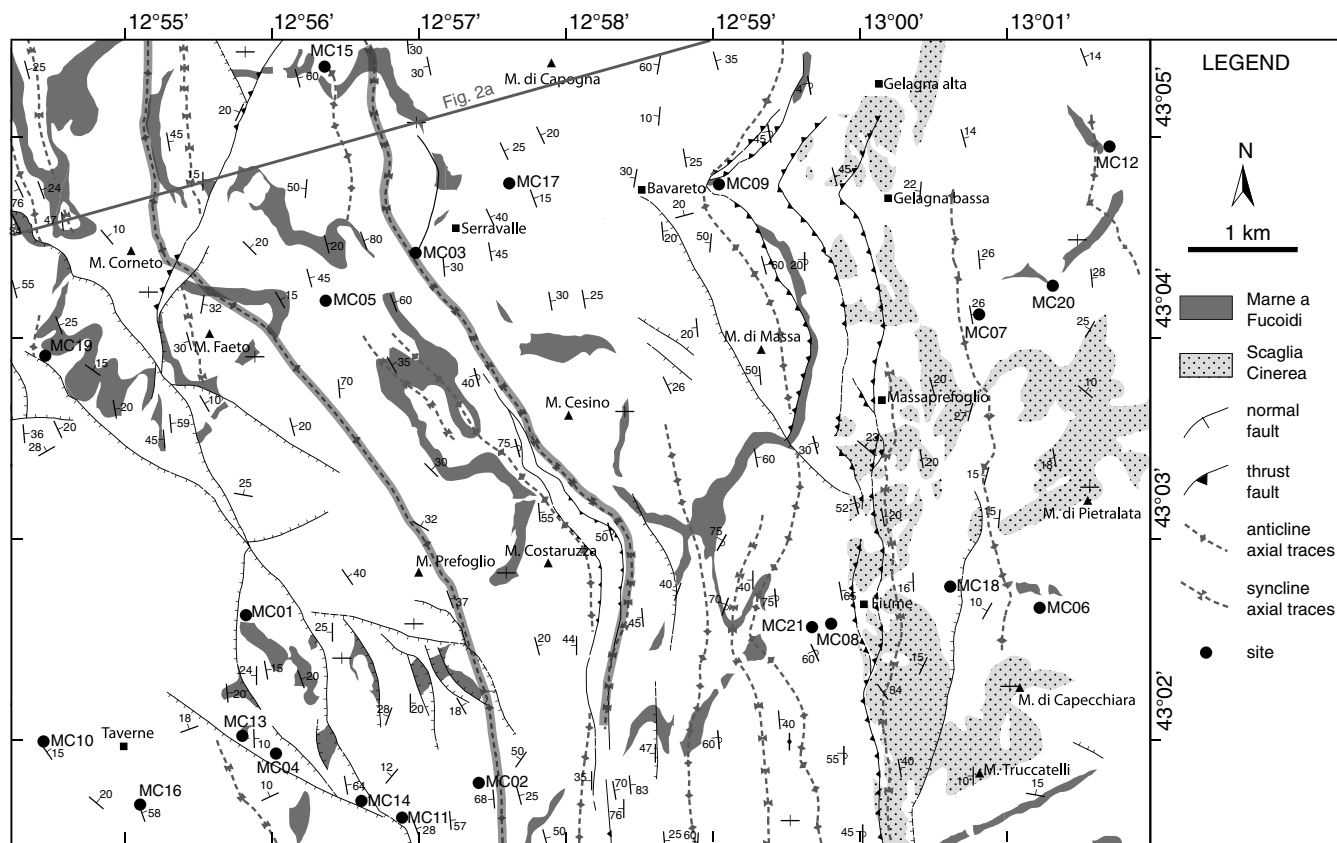


Fig. 3. Structural map of the study area; the Mount Corneto – Mount Prefoglio anticline and Mount Cesino syncline are highlighted with a thick grey line.

Here, lower Jurassic normal faults that controlled the deposition of a Jurassic condensed succession, syn-orogenic normal faults connected to the foredeep flexural domain (Scisciani *et al.* 2000) and post-orogenic W-dipping normal fault systems that control the present-day seismic activity (Calamita & Pizzi, 1994; Calamita *et al.* 2000) can be recognized.

We performed a detailed palaeomagnetic and structural analysis from 21 sites in order to investigate the relation between vertical axis rotations and fold axial trend and unravel the kinematic mechanism acting in local arcuate structure.

The age of sites was established through microfossil assemblage analysis of thin sections, with the exception of barren sites (MC01, MC02, MC05, MC14 and MC15) whose age was extrapolated from geological maps (Barchi *et al.* 2012). Sites are mainly collected in the Scaglia Rossa and Scaglia Bianca formations: seven sites from the upper Cretaceous (MC04, MC07, MC10, MC13, MC16 and MC20) and Eocene (MC08) Scaglia Rossa Formation; five sites from the Scaglia Bianca Formation (MC03, MC06, MC09, MC12 and MC19). Another five sites were collected from the Upper Tithonian – Lowermost Aptian Maiolica Formation (MC02, MC05, MC14, MC15 and MC17), three sites from the Upper Albian part of the Marne a Fucoidi Formation (MC01 and MC20 in the reddish member V and MC18 in the white member VI (Coccioni *et al.* 1989), and one site in the Bajocian–Tithonian Calcari Diasprigni Formation (MC11).

3.a. Structural analysis

A structural analysis was performed with the aim of constraining the fold axial trend of the macrofolds recognized from the available

geological cartography (Barchi *et al.* 2012). In order to outline the axial trace of the anticlines and synclines, the Marne a Fucoidi and Scaglia Cinerea formation limits have been traced together with bedding values. In fact, due to their relative reduced thickness, these two formations provide a clear marker of the outcropping structures (Fig. 3).

Apennine folds approximate cylindrical folds when observed at the outcrop scale, even when en échelon arrangement is observed at regional scale. In fold and thrust belts, pressure-solution cleavage sub-orthogonal to the bedding is associated with pre-folding layer parallel shortening (Tavernelli, 1997; Fossen, 2010; and references therein). In the study area, the stylolitic pressure-solution cleavage, evident in meso-folded beds, realizes with the bedding an intersection lineation (S_0/S_1) parallel to the axial trend of folds. As a consequence, fold axial trends of the study area have been reconstructed using π - and β -diagrams integrated with the lineation (S_0/S_1).

The hinges of parasitic minor folds, parallel to the host main fold, have been used to infer the axial trend of major folds (Fig. 4). When exposed, the hinges have been measured in the field as linear elements; otherwise, their trend and plunge was inferred by plotting the intersection of the minor fold limbs on a stereographic projection (β -diagrams). Also, stylolitic planes of pressure solution cleavage affecting the minor folds provide information about the main fold trend. Usually, the cleavage planes (S_1) are radially arranged around the minor fold axial trend. The intersection between the cleavage planes' cyclographic projection on a stereographic diagram indicates the minor fold hinge and subsequently the axial trend of the main folds. Nevertheless, minor folds are often partially or poorly exposed

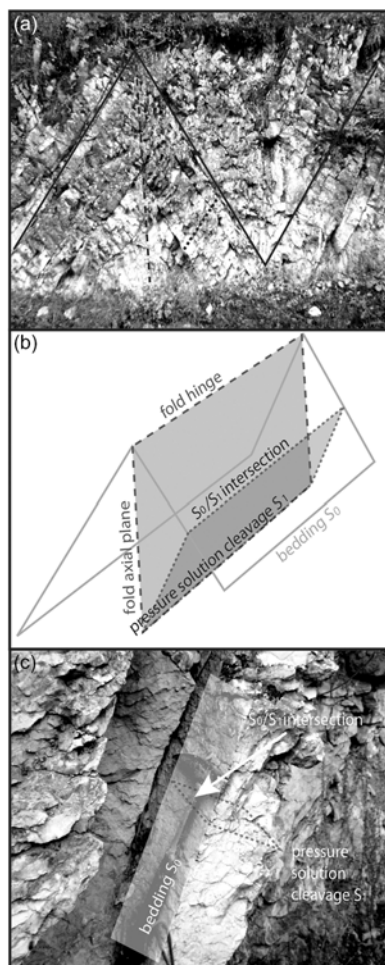


Fig. 4. Examples of measured mesoscopic structural features: (a) parasitic chevron folds from site MC02; (b) sketch of (a) highlighting the fold architecture with bedding, fold axial plane, pressure solution cleavage and the intersection line between bedding and cleavage (S_0/S_1); (c) intersection line S_0/S_1 from site MC08.

across the succession, and therefore the easiest way to define the fold trend is by measuring the bedding/cleavage intersection (S_0/S_1). Indeed, the lineations resulting from the S_0/S_1 are parallel to the host fold axial trend and therefore provide a measure of it at the outcrop scale. All the studied sites are extensively affected by pressure-solution cleavage, and the S_0/S_1 lineations are widespread, including where minor folds are poorly developed. Depending upon the lithology, the cleavage changes in term of frequency and spacing (Alvarez, 1990): calcareous formations have wider-spaced cleavage with respect to formations with higher marl content.

Data from the literature (Barchi *et al.* 2012) have been integrated with data collected from each site, including mesoscopic syn-orogenic compressional structures, as beddings (S_0), minor folds hinges and bedding-cleavage lineations (S_0/S_1), and projected on equal-area stereographic plots in order to draw π -diagrams, where the pole to the plane enveloping all the bedding poles represents the fold axis (Fig. 5). The mesostructural analysis produced 21 equal-area stereographic diagrams (Fig. 5a). In five sites, parasitic folds were well exposed and allowed computation of π -diagrams at the site scale. The stereographic diagrams led to the identification of the average fold axial trends at each site.

The structural analysis evidences a great variability of the fold axis orientation, with differences up to c. 50° (N–S vs NW–SE), comparable with the axial trend of the Mount Corneto – Mount Prefoglio anticline and Mount Cesino syncline (Fig. 5a). Due to this variability, the differences in the structural trend are strongly smoothed when grouping the sites in two domains (Fig. 5b): a N–S- (including sites MC02, MC06, MC07, MC08, MC09, MC12, MC15, MC17, MC18, MC20, MC21) and a NNW–SSE-trending group (including sites MC01, MC03, MC04, MC05, MC10, MC11, MC13, MC14, MC16, MC19).

3.b. Palaeomagnetic sampling and analysis

Palaeomagnetic sampling was performed during winter 2009/10 using a petrol-powered portable drill. Cores were oriented *in situ* by a magnetic compass, corrected to account for the magnetic declination in the analysed area ($+2.1^\circ$ according to the International Geomagnetic Reference Field; Thébaud *et al.* 2015). A total of 297 cylindrical samples (25 mm in diameter) were gathered, collecting 9–31 oriented cores (14 on average) from each site, spread laterally and vertically in the outcrop to average out secular variation of the geomagnetic field. The cores were cut into standard cylindrical specimens, and their Natural Remanent Magnetization (NRM) was measured using a 2G DC-SQUID cryogenic magnetometer in the magnetically shielded room of Istituto Nazionale di Geofisica e Vulcanologia in Rome (Italy). All samples were progressively thermally demagnetized in 15 steps between 20°C and 670°C using an ASC Model TD48 thermal demagnetizer.

3.b.1. Demagnetization behaviour

Demagnetization data were plotted on both orthogonal demagnetization diagrams (Zijderveld, 1967) and on equal-area projections. The intensity of NRM at room temperature and the demagnetization behaviour were strongly dependent upon the sampled lithologies. Samples from the Calcari Diasprigni Formation (site MC11) show very low NRM intensity at room temperature, (mean of $1.05 \times 10^{-5} \text{ A m}^{-1}$), that become indistinguishable from the noise level of the magnetometer (i.e. less than 10^{-6} A m^{-1} for a 10 cm^3 volume rock) during the demagnetization (Fig. 6a). They show unstable directions leading to inconsistent measurements and inability to determine their characteristic component of magnetization (ChRM). Samples from the Maiolica Formation are characterized by low intensity of NRM (mean of $3.87 \times 10^{-5} \text{ A m}^{-1}$), but they usually show a ChRM passing through the origin removed at a maximum temperature of 580°C (Fig. 6b, c), with the exception of eight samples for which stable endpoints were not obtained and for which remagnetization circles were analysed to obtain indications of palaeomagnetic directions. Samples from Marne a Fucoidi whitish member VI (Fig. 6e) and from the Scaglia Bianca Formation (Fig. 6g, i) show similar NRM values ($3.06 \times 10^{-4} \text{ A m}^{-1}$ and $5.1 \times 10^{-4} \text{ A m}^{-1}$, respectively) and are generally completely demagnetized between 540°C and $580\text{--}620^\circ\text{C}$. The higher NRM values ($2.91 \times 10^{-3} \text{ A m}^{-1}$ and $1.88 \times 10^{-3} \text{ A m}^{-1}$, respectively) are from samples from Marne a Fucoidi reddish Member V (Fig. 6d, f) and Scaglia Rossa formations (Fig. 6j, k) that are usually completely demagnetized between 580°C and 670°C .

The unblocking temperature spectra observed during thermal cleaning (Curie temperature close to 580°C) indicate that the remanence is mainly carried by minerals of the magnetite and titanomagnetite family in samples from the Maiolica

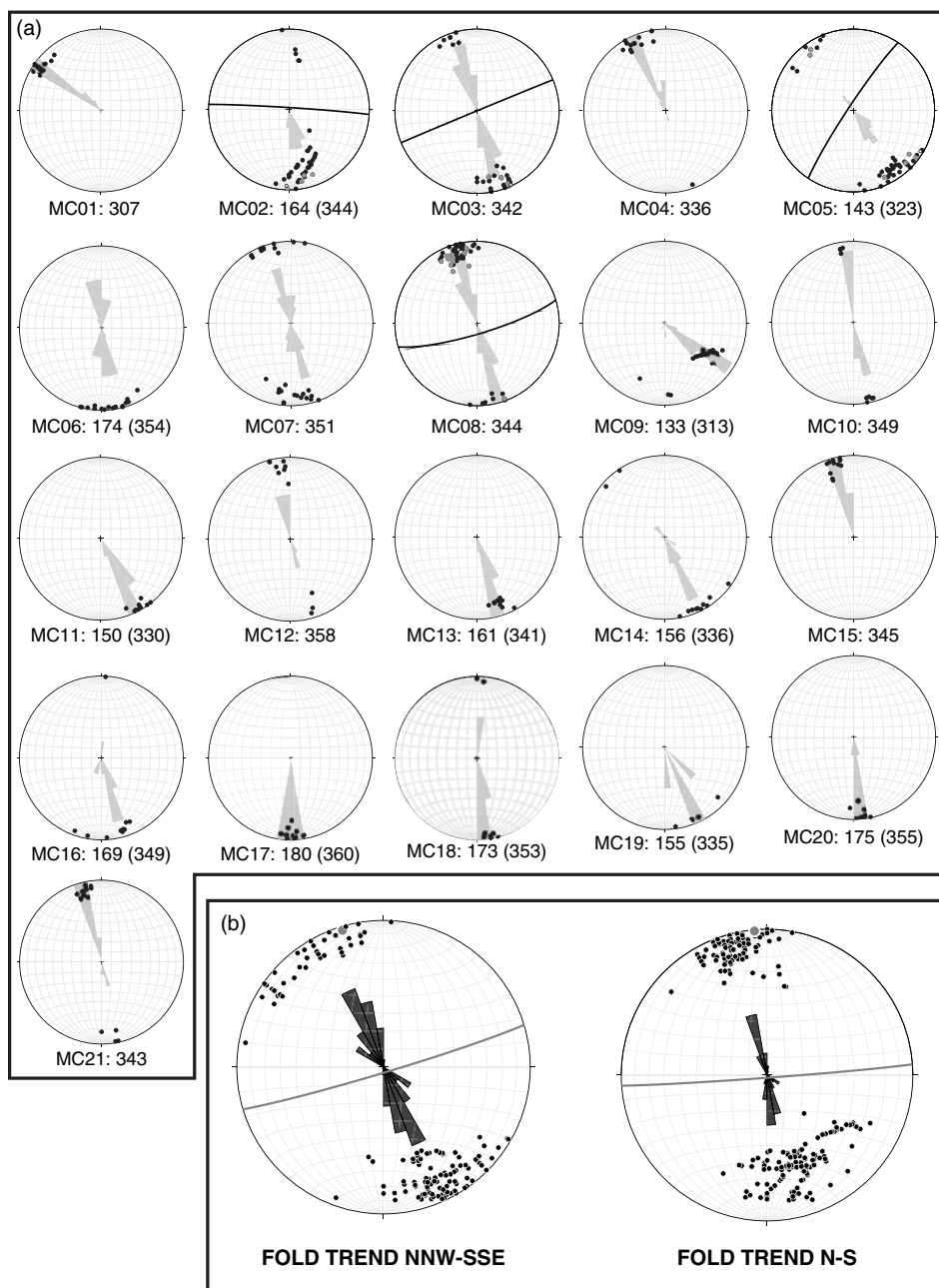


Fig. 5. Equal-area stereographic projections of the structural data. (a) Rose diagrams of cleavage-bedding lineations S_0/S_1 (black dots) and mesoscopic fold hinges (grey circles); white dots indicate the fold axis computed as the pole to the plane (black line) enveloping all the bedding poles. Numbers indicate the structural fold axial trend derived by S_0/S_1 intersection lineations, meso-fold hinges and π -diagram. (b) Synthetic structural analysis of the NNW-SSE and N-S trends. Black dots indicate S_0/S_1 lineations and fold hinges gathered from each site; the grey dots and circles are the results of the π -diagrams enveloping all the bedding poles. A smaller cluster in the histogram at 120° is due to site MC09, located on a thrust fault that could have yielded very local rotations.

Formation, while some samples from Scaglia Bianca, Scaglia Rossa and Marne a Fucoidi formations show unblocking temperatures exceeding 620°C , indicating the presence of hematite in addition to magnetite. Specific analyses for the magnetic mineralogy performed on rocks from the same formations can be found in the literature (e.g. Tarduno *et al.* 1992; Channell & McCabe, 1994; Caricchi *et al.* 2014; Satolli & Turtù, 2016).

3.b.2. Magnetization components

Remanence magnetization components were isolated by principal component analysis (Kirschvink, 1980) or estimated by using

remagnetization circles when components with overlapping demagnetization spectra were observed. Almost all samples are characterized by the presence of at least two out of the following three observed magnetization components (Fig. 6): 1. A low blocking temperature component; 2. An intermediate-temperature (ITC); 3. A ChRM isolated after the removal of the low-blocking temperature component or ITC. The mean directions were computed using either Fisher's (1953) statistics, where only magnetization components were well isolated, or the McFadden & McElhinny (1988) method to combine direct observations with remagnetization circles, by using Paleomac software (Cogné, 2003).

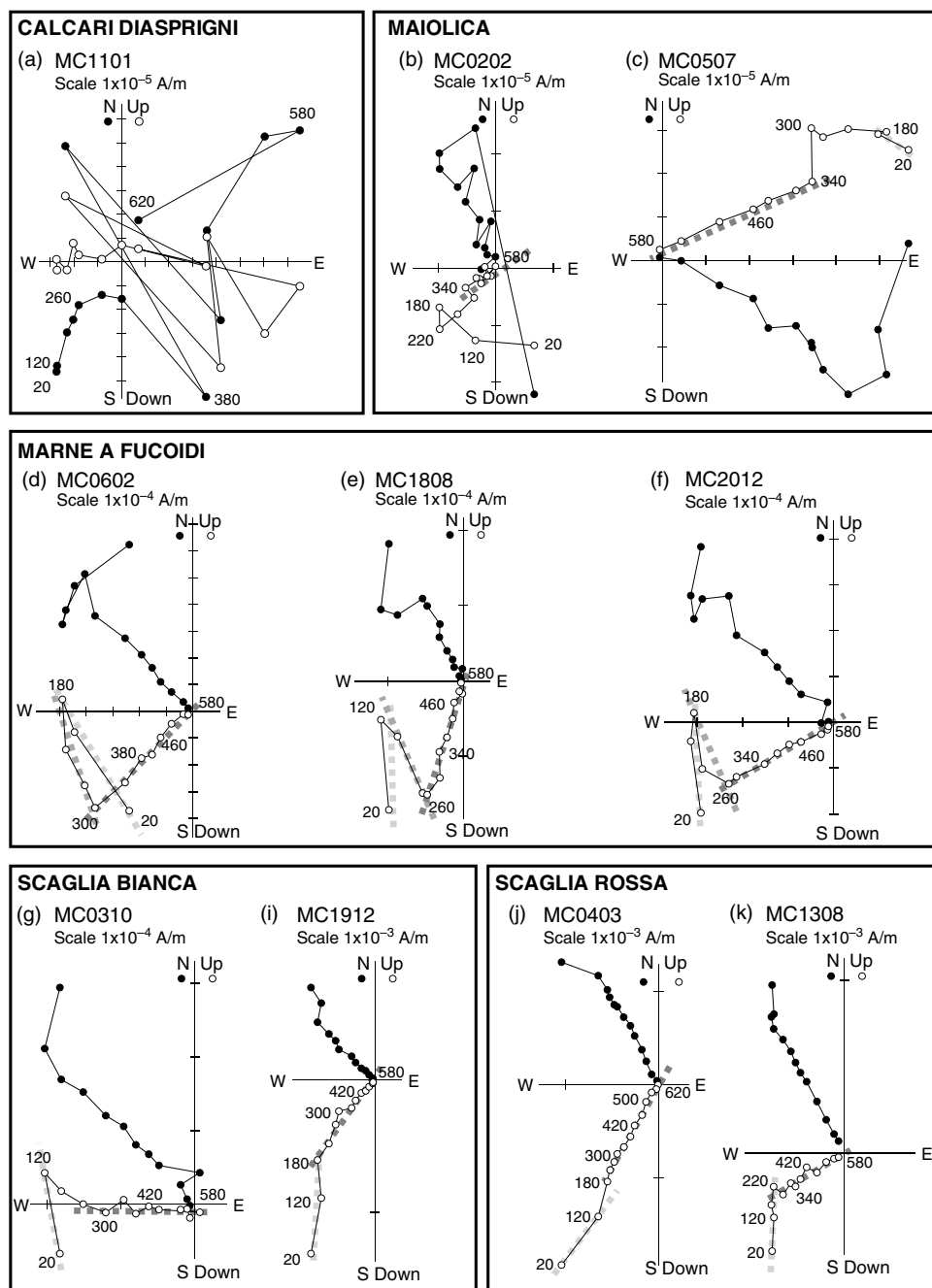


Fig. 6. Vector diagrams of typical demagnetization data, *in situ* coordinates, showing the demagnetization behaviour of the different sampled lithologies: Calcari Diasprigni Formation (a) with scattered data that hampered the isolation of the characteristic remanent magnetization; Maiolica (b, c) and Marne a Fucoidi formations (d–f) showing stable characteristic remanent magnetization up to 580 °C or 670 °C; Scaglia Bianca (g–i) and Scaglia Rossa (j–l) formations. Dark, medium and light grey indicate the characteristic remanent magnetization, the intermediate temperature component and the viscous component, respectively. Open (solid) symbols represent projection onto the vertical (horizontal) planes. Demagnetization steps values are expressed in °C.

The low blocking temperature (Table 1) component is isolated between room temperature and 180–220 °C in almost all samples (282 over 297). It always shows normal polarity in *in situ* coordinates ($D = 358.5^\circ$, $I = 58.0^\circ$, $\alpha_{95} = 2.9^\circ$) while it shows mixed polarities in tilt-corrected coordinates ($D = 9.8^\circ$, $I = 46.5^\circ$, $\alpha_{95} = 5.5^\circ$). In *in situ* coordinates this component corresponds to the Geocentric Axial Dipole (GAD) field direction expected at the sampling locality ($D = 0^\circ$, $I = 61.8^\circ$). As a consequence, the low-temperature component was interpreted as a viscous overprint acquired during the Brunhes polarity chron.

The ITCs are isolated between 120–180 °C and 260–340 °C in 65 samples from five sites (MC06, MC09, MC12 from Scaglia Bianca and MC18, MC20 from Marne a Fucoidi; Fig. 6). For these sites, the mean ITC directions (Table 1; Fig. 7) are well grouped before bedding correction ($D = 225.9^\circ$, $I = -66.5^\circ$, $\alpha_{95} = 4.4^\circ$); conversely data are more scattered after the tectonic correction ($D = 245.6^\circ$, $I = -35.4^\circ$, $\alpha_{95} = 10.2^\circ$).

The ChRMs are isolated in different temperature ranges, depending upon the lithology and the presence of the ITC, between 180–300 °C and 580–670 °C (Table 2; Fig. 7). They were defined for

Table 1. Low- and intermediate-temperature components of magnetization

| Low-temperature component | | | | <i>In situ</i> | | Tilt-corrected | | | |
|------------------------------------|---------------------------------------|----------------------|---------------------------|----------------|-----------------|----------------|-----------------|----------------|-----------------|
| Site | Age | <i>n/N</i> | <i>T</i> (°C) | <i>D I</i> | $\alpha_{95} k$ | <i>D I</i> | $\alpha_{95} k$ | | |
| ALL | | 282/297 | 20–220 | 358.5 | 2.9 | 9.8 | 5.5 | | |
| | | | | 58.0 | 9.2 | 46.5 | 3.3 | | |
| Intermediate-temperature component | | | | | | <i>In situ</i> | | Tilt-corrected | |
| Site | Coordinates | Formation | Age | <i>n/N</i> | <i>T</i> (°C) | <i>D I</i> | $\alpha_{95} k$ | <i>D I</i> | $\alpha_{95} k$ |
| MC06 | 43° 02' 36.50" N, 13° 01' 31.04" E | Scaglia Bianca | Upper Albian – Cenomanian | 14/14 | 180–260 | 225.8 | 5.3 | 258.5 | 6.2 |
| | | | | | | –69.5 | 57.4 | –58.5 | 42.1 |
| MC09 | 43° 04' 35.94" N, 12° 58' 58.38" E | Scaglia Bianca | Turonian | 8/13 | 180–300 | 223.2 | 15.5 | 219.0 | 16.8 |
| | | | | | | –55.4 | 13.7 | 50.5 | 11.8 |
| MC12 | 43° 04' 49.00" N, 13° 01' 42.00" E | Scaglia Bianca | Albian–Cenomanian | 20/21 | 120–300 | 220.6 | 10.8 | 248.1 | 11.4 |
| | | | | | | –71.6 | 10.1 | –13.1 | 9.2 |
| MC18 | 43° 02' 34.00" N, 13° 00' 58.00" E | Marne a Fucoidi (VI) | Upper Albian – Cenomanian | 12/13 | 120–260 | 227.2 | 11.2 | 219.1 | 11.4 |
| | | | | | | –66.8 | 16.0 | –68.5 | 15.4 |
| MC20 | 43° 04' 19.00" N, 13° 01' 32.00" E | Marne a Fucoidi (V) | Upper Albian | 11/14 | 180–260 | 232.7 | 6.4 | 257.8 | 6.5 |
| | | | | | | –61.2 | 51.5 | –45.1 | 50.4 |
| Mean | | | | | | 225.9 | 4.4 | 245.6 | 10.2 |
| | | | | | | –66.5 | 16.8 | –35.4 | 3.9 |

n/N: number of reliable samples with respect to the total number of samples; *T* (°C): temperature range in which magnetization components were isolated; *D* and *I*: site-mean declination and inclination; *k* and α_{95} : statistical parameters after Fisher (1953).

all sites with the exception of site MC11, sampled in the Calcare Diaprigni Formation. For 232 of the 298 measured samples the ChRMs are defined by a vector passing through the origin, while for 9 samples (8 samples from Maiolica and 1 sample from the Scaglia Bianca Formation) only remagnetization circles could be calculated. Both the *in situ* and the tilt-corrected mean ChRMs are far from the GAD field direction expected in the study area, thus generally excluding the possibility of a recent magnetic overprint, with the exception of sites MC14 and MC15, whose semi-angle of confidence overlaps with the GAD field in *in situ* coordinates (Fig. 7). The site-mean directions are always more clustered in tilt-corrected coordinates (even if in most cases bedding variations are too small to successfully perform a fold test) (Table 2), supporting a pre-folding acquisition of the magnetization.

3.b.3. Magnetization reliability tests

Fold (McFadden, 1990) and reversal (McFadden & McElhinny, 1990) tests were performed on both ITCs and ChRM components (Fig. 8).

The ChRMs show both normal and reverse polarity directions after tilt correction, though the normal polarities are predominant, save for site MC17 only showing reverse polarities (Table 2). When considering all directions in normal polarity, the palaeodeclinations are spread from N to W. Given such great declinational scatter, it was not possible to perform the fold and the reversal tests on the whole set of site mean directions. However, an inclination-only fold test (Enkin & Watson, 1996) was performed on all ChRMs and indicates that magnetization was acquired at 115.0 % of unfolding (*I* = 36.7°, α_{95} = 1.8°, *k* = 25.68) suggesting that ChRMs are acquired pre-folding, when bedding was horizontal. Furthermore, the small bedding variations are unfavourable for a fold test to be applied at site level, save for sites MC02 and

MC03 that were sampled in the limbs of metric-scale folds. The fold test is inconclusive for site MC02 (although *k*_{max} = 16.9 is observed at 100 % of complete unfolding; Fig. 8a) and positive at 99 % significance level for site MC03 (Fig. 8b).

The reversal test was performed on sites showing both normal and reverse polarity ChRMs (MC02, MC05, MC08, MC09 and MC10). It is positive of class C for sites MC02 (γ = 10.2 and γ_c = 17.4, where γ is the angle between the mean normal and reverse directions and γ_c is its critical angle; Fig. 8a) and MC05 (γ = 9.7 and γ_c = 10.4; Fig. 8c), while it is indeterminate for sites MC08, MC09 and MC10 (Fig. 8d–f).

As sites carrying the ITCs are similar in age, it was possible to perform the fold test using the mean direction from all sites. The fold test (McFadden, 1990) is negative, with maximum *k* observed at 5 % of complete unfolding (*k*_{max} = 18.0). These results indicate a post-folding age of magnetization acquisition. For this reason, ITCs are not used to evaluate rotations in the study area. A similar ITC has been documented in other sites and sections from the Northern Apennines (e.g. Tarduno *et al.* 1992; Aiello *et al.* 2004; Satolli *et al.* 2007, 2008). The pole position indicates the remagnetization was acquired during a Tertiary reversed polarity chron. However, its origin is still unclear: among other causes, it may be due to the Messinian – Lower Pliocene burial of the chain (e.g. Satolli *et al.* 2008), or to external derived fluids (e.g. enhanced circulation of orogenic fluids during the uplift; Lu *et al.* 1990; Aiello *et al.* 2004).

3.b.4. Comparison with the expected directions

In order to evaluate the presence of tectonic rotations related to thrust sheet emplacement of local arcuate structures in the inner part of the Northern Apennines second-order arc, the obtained tilt-corrected palaeomagnetic directions were compared to coeval directions expected for the Adriatic foreland. As Adria is

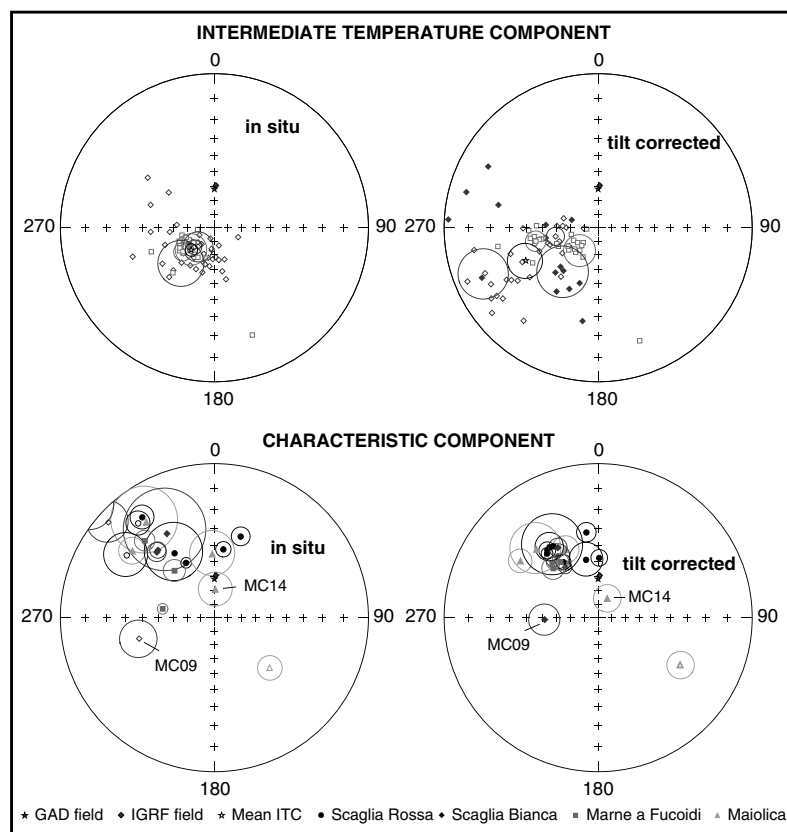


Fig. 7. Equal-area projections of palaeomagnetic data. Solid (open) symbols represent projections onto the lower (upper) hemisphere. Open ellipses are the projections of the α_{95} . Sites MC09 and MC14 indicated in the Characteristic Component plot were discarded from tectonic considerations.

considered to have mirrored African drift since at least Permian times (Channell, 1992; Van der Voo, 1993; Muttoni *et al.* 2001; Satolli *et al.* 2007, 2008), declination and inclination values were compared to the African palaeopoles from Besse & Courtillot (2002). The rotation and flattening values were computed according to Demarest (1983), using the reference palaeopole closer to the site mean age.

The mean ChRMs show differences with the expected directions (R in Table 2) that are interpreted as rotations around the vertical axis induced by movement of rigid crustal blocks during Apennine orogenesis (according to Speranza *et al.* 1997; Satolli *et al.* 2005). The rotations strongly vary in sign and magnitude, with a mean value of 7.6. The mean flattening value is 3.96, with 50 % of samples included between 0.75 and 11.95. Flattening values are in agreement with shallow palaeomagnetic inclinations reported in the literature from the Apennines (e.g. Satolli *et al.* 2007, 2008) and attributed to the effects of shallowing and diagenesis (e.g. Deamer & Kodama, 1990). Two sites are characterized by strong rotations and/or significantly negative flattening value (site MC09 with 72.5° CCW rotation and site MC14 with 66.9° CW rotation and -35.8 of flattening). These sites show other evidence for non-primary magnetization. The Turonian site MC09 is characterized by mixed polarities that are implausible in the long normal Cretaceous superchron and show an *in situ* component similar to the ITC component, so it may have been overprinted by it; also, it is located close to a thrust fault that could have yielded very local rotations. Site MC14 is characterized by a semi-angle of confidence overlapping with the GAD field in *in situ* coordinates, suggesting a possible viscous overprint. On the basis of these

considerations, sites MC09 and MC14 were excluded from tectonic implications.

3.b.5. Analysis of the primary nature of ChRMs

Given their ages, the magnetic polarities in tilt-corrected coordinates were compared to their expected polarity from the geomagnetic polarity timescales (Gradstein *et al.* 2012). The comparison revealed that sites found entirely within the long normal Cretaceous superchron consistently show normal polarity (i.e. sites MC01, MC03, MC04, MC06, MC12, MC18, MC19, MC20), save for the Turonian site MC09 that shows reversed polarities. A direct comparison with the geomagnetic polarity timescale was not possible for other sites, as their age intervals encompass several polarity chrons.

Considering the reliability criteria of the palaeomagnetic data (Van der Voo, 1990, 1993; Pueyo *et al.* 2016), several lines of evidence support the primary nature of the ChRMs: 1. Data are always more clustered in tilt-corrected coordinates (save for site MC09), suggesting an acquisition of the magnetization before folding (Table 2); 2. ChRMs show both normal and reverse polarities (Figs 7, 8; Table 2); 3. Both the *in situ* and tilt-corrected palaeomagnetic directions are far from the GAD field direction (Fig. 7), suggesting the absence of magnetic overprints (save for sites MC14 and MC15, *in situ* coordinates); 4. Sites with biostratigraphic ages entirely falling within the long normal Cretaceous superchron consistently show a normal polarity; 5. Observed inclinations (Table 2) are generally in agreement with the expected inclinations for the Adriatic/African foreland (save for site MC14 that shows a significant scatter); 6. The inclination-only fold test is consistent with

Table 2. Characteristic component of magnetization and tectonic rotations from the sampled sites

| Site | Coordinates | Formation | Age | η/N | T (°C) | Characteristic component of magnetization | | | $R F$ | |
|--------------------|---------------------------------------|-------------------------|---|----------|----------|---|-----------------|----------------|-----------------|--------------|
| | | | | | | $D I$ | $\alpha_{95} k$ | Tilt-corrected | | |
| | | | | | | $D I$ | $\alpha_{95} k$ | $D I$ | $\alpha_{95} k$ | |
| MC01 ^m | 43° 02' 38.71" N, 12° 55' 53.94" E | Marne a Fucoidi (V) | Upper Albian | 13/13 | 300–670 | 279.7 | 3.5 | 320.0 | 3.5 | -14.4 ± 22.6 |
| MC02 ^m | 43° 01' 33.13" N, 12° 57' 33.02" E | Maiolica | Upper Tithonian p.p. – Lower Aptian p.p. | 21/31 | 300–580 | 52.4 | 138.9 | 40.2 | 138.9 | 3.7 ± 25.7 |
| MC03 | 43° 04' 11.48" N, 12° 56' 56.35" E | Scaglia Bianca | Upper Albian – Cenomanian | 11/12 | 180–580 | 330.5 | 21.5 | 326.4 | 7.6 | -12.7 ± 9.6 |
| MC04 | 43° 01' 36.58" N, 12° 56' 14.43" E | Scaglia Rossa | Turonian | 12/13 | 260–620 | 332.7 | 3.4 | 321.4 | 3.4 | -19.0 ± 4.4 |
| MC05 ^m | 43° 03' 57.63" N, 12° 56' 26.92" E | Maiolica | Upper Tithonian p.p. – Lower Aptian p.p. | 8/12 | 260–580 | 309.1 | 6.8 | 306.1 | 6.3 | -12.3 ± 7.2 |
| MC06 | 43° 02' 36.50" N, 13° 01' 31.04" E | Scaglia Bianca | Upper Albian – Cenomanian | 14/14 | 300–670 | 320.1 | 4.6 | 327.0 | 4.2 | -11.4 ± 11.1 |
| MC07 | 43° 03' 58.46" N, 13° 00' 44.86" E | Scaglia Rossa | Campanian – Maastrichtian | 8/12 | 220–670 | 17.9 | 5.4 | 1.0 | 5.4 | 13.6 ± 9.1 |
| MC08 | 43° 02' 25.17" N, 12° 59' 51.37" E | Scaglia Rossa | Middle Eocene | 10/13 | 260–670 | 305.4 | 10.9 | 348.2 | 10.9 | -10.1 ± 13.7 |
| *MC09 | 43° 04' 35.94" N, 12° 58' 58.38" E | Scaglia Bianca | Turonian | 12/13 | 340–580 | 254.5 | 11.0 | 267.9 | 10.3 | -72.5 ± 13.4 |
| MC10 | 43° 01' 44" N, 12° 54' 29" E | Scaglia Rossa | Campanian– Maastrichtian | 8/9 | 260–620 | 328.2 | 17.2 | 327.9 | 17.2 | -19.5 ± 17.3 |
| *MC11 | 43° 01' 22" N, 12° 56' 57" E | Diaspri | Lower Bajocian p.p. – Lower Tithonian p.p. | 0/12 | | 37.7 | 11.3 | 32.7 | 11.3 | 15.0 ± 15.0 |
| MC12 | 43° 04' 49" N, 13° 01' 42" E | Scaglia Bianca/Rossa | Albian– Cenomanian | 18/21 | 260–620 | 312.0 | 8.3 | 325.5 | 8.0 | -13.6 ± 9.3 |
| MC13 | 43° 01' 40" N, 12° 56' 08" E | Scaglia Rossa | Upper Turonian p.p. – Santonian | 14/14 | 220–580 | 324.3 | 5.4 | 322.9 | 4.8 | -17.5 ± 5.3 |
| *MC14 ^m | 43° 01' 24" N, 12° 56' 53" E | Maiolica | Upper Tithonian p.p. – Lower Aptian p.p. | 7/11 | 120–580 | 1.7 | 12.1 | 25.3 | 10.0 | 66.9 ± 31.5 |
| MC15 ^m | 43° 05' 13" N, 12° 56' 15" E | Maiolica | Upper Tithonian p.p. – Lower Aptian p.p. | 12/15 | 180–525 | 358.0 | 14.2 | 317.9 | 13.8 | -0.5 ± 13.1 |
| MC16 | 43° 01' 19" N, 12° 55' 18" E | Scaglia Rossa | Coniacian– Santonian | 14/15 | 220–580 | 7.5 | 4.7 | 328.0 | 4.7 | -9.1 ± 10.1 |
| | | | | | | 41.8 | 71.1 | 43.9 | 71.1 | 4.1 ± 9.7 |

(Continued)

Table 2. (Continued)

| Site | Coordinates | Formation | Age | n/N | T (°C) | Characteristic component of magnetization | | | Tilt-corrected | | | R F |
|------|---------------------------------|-------------------------|------------------------------|-------|---------|---|-----------------|------|----------------|-----------------|--------------|-----|
| | | | | | | In situ | | | | | | |
| | | | | | | D I | α_{95} k | | D I | α_{95} k | | |
| MC17 | 43° 04' 36" N, 12° 57' 35" E | Maiolica | Berriasian | 11/15 | 340–580 | 132.2 | 7.4 | 7.4 | 119.9 | 7.4 | –12.2 ± 11.6 | |
| MC18 | 43° 02' 34" N, 13° 00' 58" E | Marne a Fucoidi (VI) | Upper Albian – Cenomanian | 12/13 | 260–580 | 319.6 | 7.1 | 39.3 | 317.6 | 7.0 | –20.8 ± 12.5 | |
| MC19 | 43° 03' 14" N, 12° 54' 55" E | Scaglia Bianca | Upper Albian | 12/13 | 220–580 | 318.7 | 5.4 | 39.5 | 330.2 | 5.4 | –8.2 ± 11.2 | |
| MC20 | 43° 04' 19" N, 13° 01' 32" E | Marne a Fucoidi (V) | Upper Albian | 12/14 | 260–580 | 317.9 | 5.3 | 65.9 | 325.8 | 5.3 | –8.7 ± 23.1 | |
| MC21 | 43° 02' 24" N, 12° 59' 42" E | Scaglia Rossa | Santonian– Maastrichtian | 11/12 | 300–620 | 22.1 | 69.1 | 69.1 | 42.9 | 69.1 | 1.0 ± 25.9 | |
| | | | | | | 321.1 | 5.5 | 5.5 | 352.1 | 5.5 | 13.5 ± 8.0 | |
| | | | | | | –13.6 | 69.3 | 69.3 | 31.7 | 69.3 | 17.0 ± 7.6 | |

^m indicates which ages were determined using map information; * indicates sites discarded from tectonic considerations; n/N: number of reliable samples with respect to the total number of samples; T (°C): temperature range in which magnetization components were isolated; D and I: site-mean declination and inclination; k and α_{95} : statistical parameters after Fisher (1953); R and F: site-mean rotation and flattening values (Demarest, 1983) relative to coeval D and I/African values expected in the study area (from Besse & Courtillot, 2002).

ChRMs acquired before folding; 7. Positive (or inconclusive) fold test at the site scale indicates a pre-folding age of magnetization acquisition; 8. Positive (or indeterminate) reversal test at the site scale indicates that magnetic overprints were removed.

All the sites satisfy at least one of these conditions. As a consequence, the ChRMs are considered to represent the primary magnetization and to be suitable for tectonic reconstruction. However, sites MC09, MC14 and MC15 show evidence of remagnetization that possibly affected the primary component and will be discussed below.

4. Relation between fold axial trends and vertical axis rotations

Rotations, given by the difference in angle between the measured primary ChRM declination and the expected declination, and fold axial trends from each site have been plotted on the geological and structural map (Fig. 9) in order to highlight their possible correlation.

The relationship between vertical axis rotations and fold axial trends has been quantitatively evaluated by analysing the pattern of rotation deviations versus structural trend deviations, according to the bootstrapped oroclinal test (Koymans *et al.* 2016; Pastor-Galán *et al.* 2017) where horizontal or unit slope best-fit lines define a non-rotational arc or a perfect oroclinal behaviour, respectively. We plotted the rotation deviation (where the reference rotation R_0 is 0) against structural deviation computed as the difference between the strike of each site and the reference structural direction from the Northern Apennines ($S_0 = F_0 = 315^\circ$, e.g. Speranza *et al.* 1997). Data are roughly aligned along a horizontal line, thus approaching a non-rotational arc behaviour. Furthermore, the coefficient of correlation close to zero proves the absence of correlation between variation in vertical axis rotations and structural trend. The lack of correlation suggests that differences in the fold axial trend that give the local arcuate shapes of the Mount Corneto – Mount Prefoglio anticline and Mount Cesino syncline are not due to a oroclinal behaviour but are mostly primary features.

5. Discussion

The oroclinal plot (Fig. 10) derived from the 18 retained sites from domains characterized by homogeneous fold trends clearly shows vertical axis rotations independent from the local curvature. In fact, the c. 50° change in the structural trend is much greater than the difference in rotation, and highlights the role of inherited structures in nucleating the structural features. Several studies document the presence of positive inversion tectonics in the Northern Apennines, with the reactivation of pre- and syn-orogenic normal faults (e.g. Di Domenica *et al.* 2012; Scisciani *et al.* 2014). The arcuate structures documented in this study are likely due to the interaction of the orogenic wedge with primary features inherited from pre-orogenic discontinuities of the Adria passive margin, only locally accentuated by the occurrence of vertical axis rotations (Fig. 11).

Conversely, the oroclinal plot of the first-order arc of the Northern Apennines arc shows that it is a progressive arc (fig. 5 from Cifelli & Mattei, 2010), where tectonic rotations have been induced during the orogenesis, accentuating a pre-existent arcuate shape. Here, the primary curvature affected by the presence of inherited discontinuities was accentuated by tectonic rotations induced by the orogenesis (e.g. Cifelli & Mattei, 2010; Satolli & Calamita, 2012; Turtù *et al.* 2013).

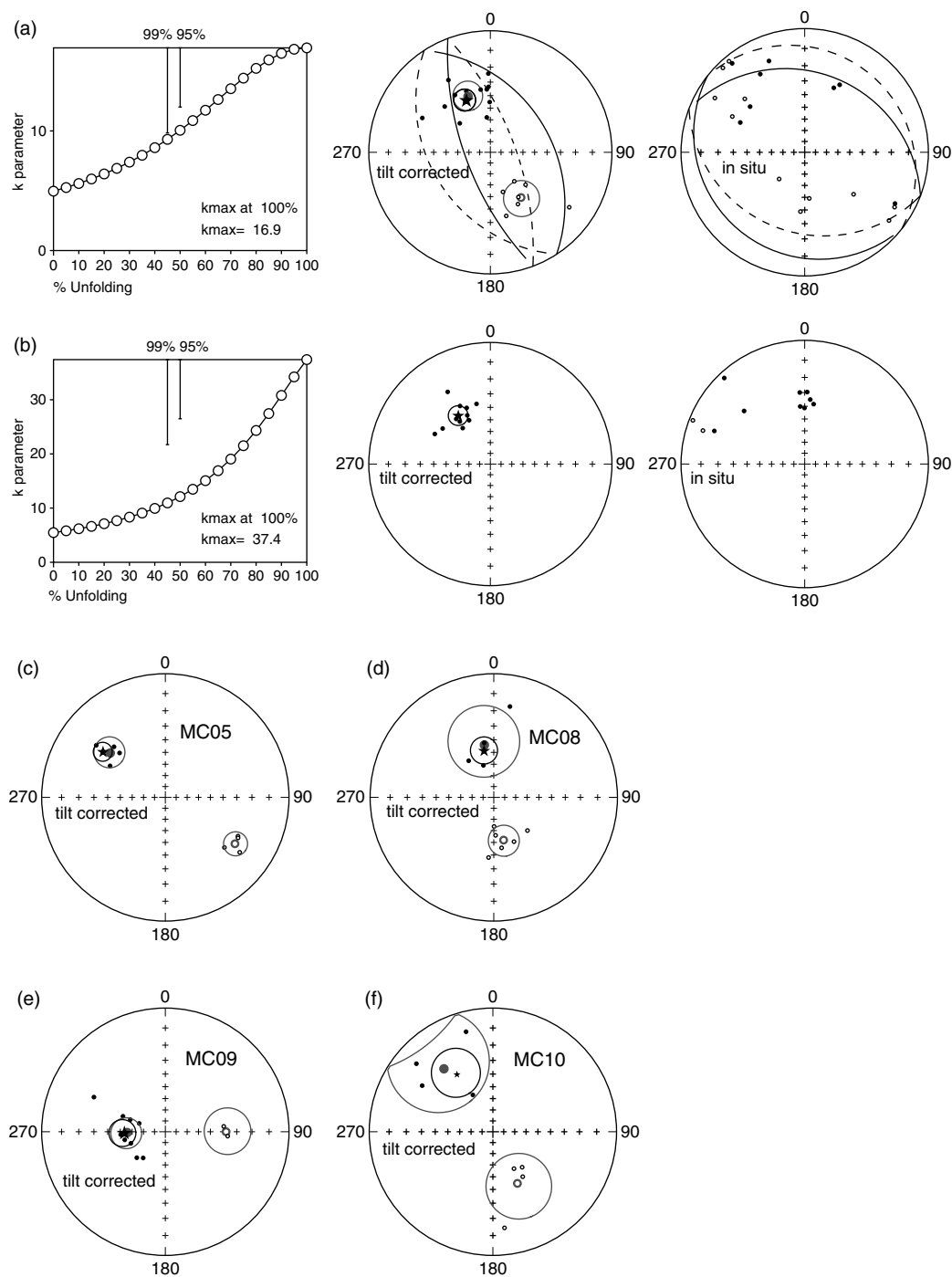


Fig. 8. Reliability test performed on palaeomagnetic data: (a) fold and reversal test for site MC02; (b) fold test for site MC03; (c–f) reversal test for sites MC05, MC08, MC09 and MC10, respectively.

These new data show that kinematics of first-order and second-order or minor arcs is markedly different, probably due to the acting of different dynamics: while the first-order arcs are likely driven by large-scale lithospheric bending (Lucente & Speranza, 2001), the kinematics of second-order and minor arcs is the consequence of processes occurring at shallower depth in the orogenic wedge (e.g. variations in sediment thickness or local obstacles (Macedo & Marshak, 1999) or pre-existing faults). In fact, second-order arcs and minor arcs are controlled by regional pre-orogenic structures (i.e. the Ancona–Anzio line for the Northern Apennines arc) and local pre-orogenic faults, respectively.

6. Conclusions

A combined palaeomagnetic analysis integrated with geological and structural study was applied to an inner sector of the Northern Apennines characterized by an arcuate shape described by the Mount Corneto – Mount Prefoglio anticline and Mount Cesino syncline, in order to characterize this local arcuate shape within the Northern Apennines arcuate structure. The geological and structural analysis highlighted for these folds the maximum change in axial trend from N–S to NW–SE. The comparison with palaeomagnetic results shows the lack of correlation between

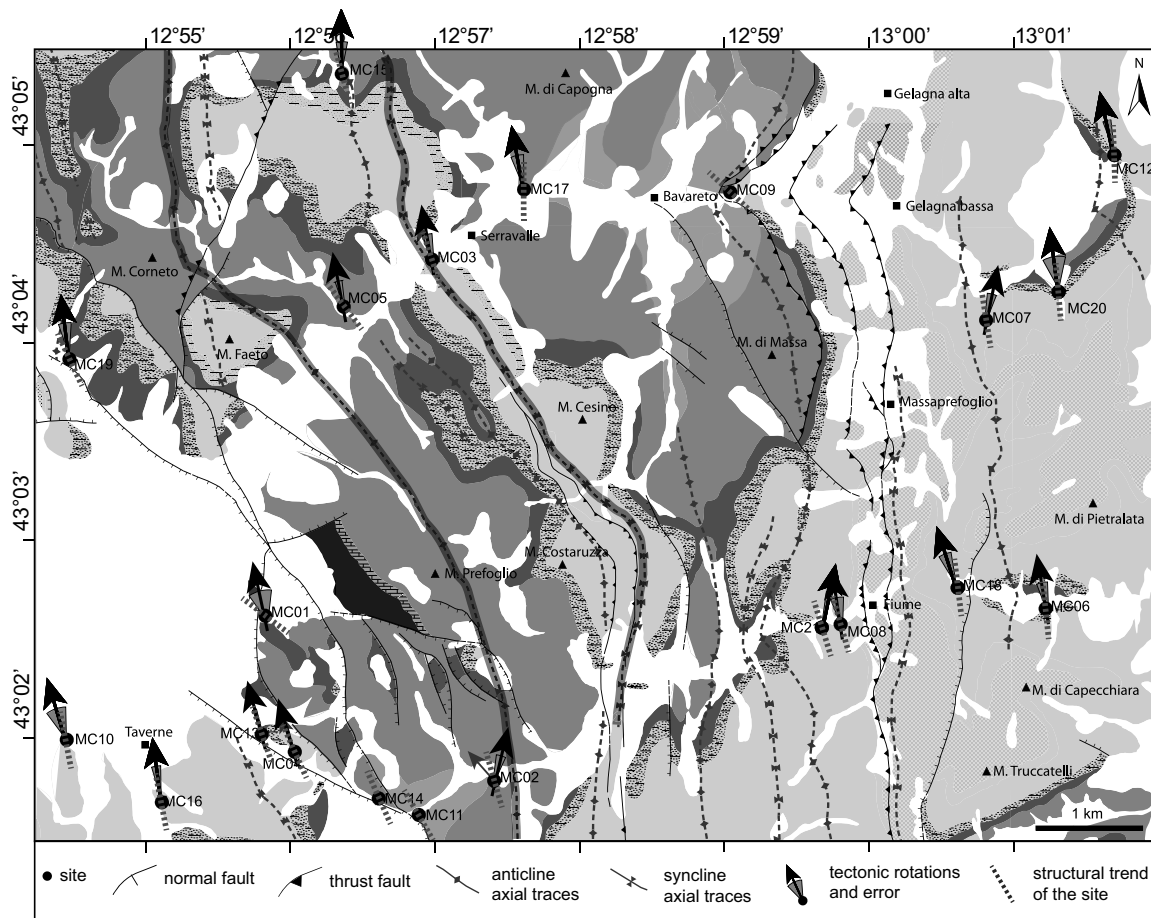


Fig. 9. Geological map of the sampled area reporting site codes and the related structural fold axial trend and tectonic rotations. See the stratigraphic column in Figure 1c for formations legend.

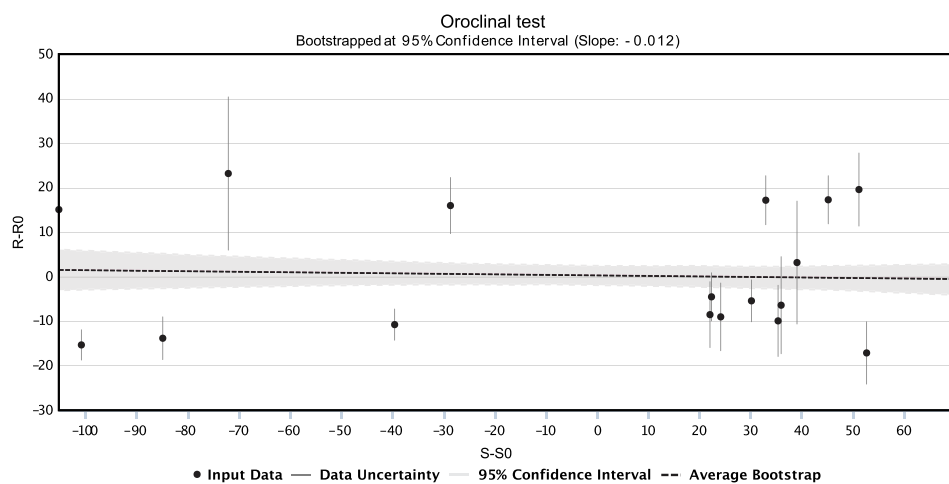


Fig. 10. Bootstrapped oroclinal test showing the rotation deviation and the structural deviation (black dots) with measurement uncertainties (grey bars). The grey line shows the total least squares regression for the data. The surrounding shaded grey area illustrates the confidence interval for 1000 bootstrapped regressions. For comparison, the average bootstrap is shown in black.

vertical axis rotations and fold axial trends. As a consequence, the minor arcuate shapes of thrusts and related folds are interpreted as mostly primary features inherited from the geometry of the palaeomargin, represented by pre-orogenic faults, according to a context of inversion tectonics.

This study highlights that the integration of palaeomagnetic and structural data is essential for understanding the kinematics of arcuate structures at different scales, and particularly the influence of inversion tectonics. The methodological approach here adopted to define the structural style of the Northern Apennines

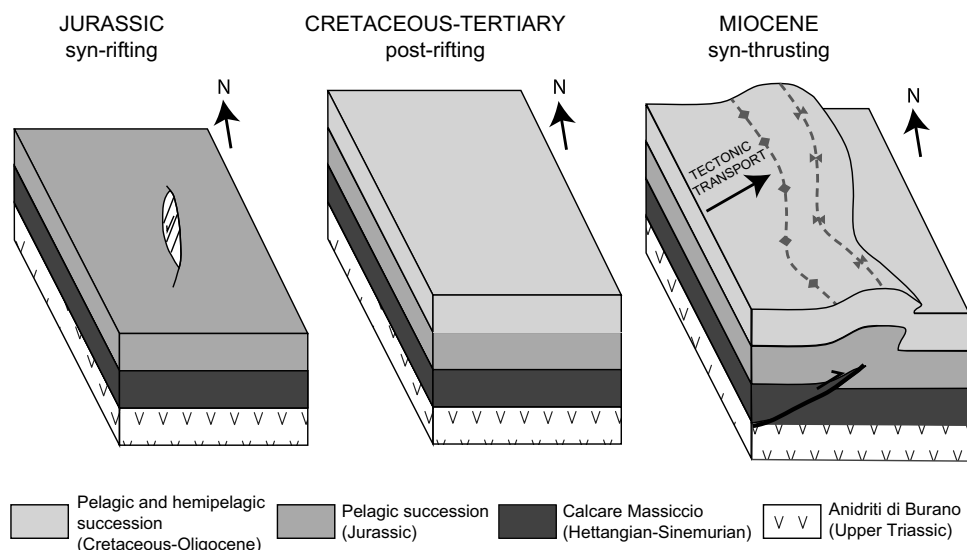



Fig. 11. Block diagram of the evolution of the study area, showing a N–S Jurassic normal fault reactivated as N–S-trending oblique blind thrust ramp and related folds within local arcuate structures in fold-and-thrust belt.

could be applied to unravel the structural style at different scales of other orogenic belts.

Author ORCIDs.  Sara Satolli [0000-0001-9848-9745](https://orcid.org/0000-0001-9848-9745), Fernando Calamita [0000-0002-1966-3061](https://orcid.org/0000-0002-1966-3061)

Acknowledgements. The authors thank the editor, O. Lacombe, the reviewer E. L. Pueyo and an anonymous reviewer for helpful comments that improved the quality of the manuscript. The authors also thank the Istituto Nazionale di Geofisica e Vulcanologia for allowing them to use the Paleomagnetic Laboratory, R. Maniscalco for thin-section analysis, A. Turtù for help in the field, and A. Rapallini, M. Clavo-Rathert and F. Speranza for comments on an earlier version of this paper. This paper was funded by FIRB – 2008 grants (grant number RBFR08GP57) of Ministero dell’Istruzione dell’Università e della Ricerca (Italy) and by MIUR grants awarded to S. Satolli and F. Calamita, respectively.

Declaration of interest. None.

References

- Aiello IW, Hagstrum JT and Principi G (2004) Late Miocene remagnetization within the internal sector of the Northern Apennines, Italy. *Tectonophysics* **383**, 1–14.
- Alvarez W (1990) Pattern of extensional faulting in pelagic carbonates of the Umbria-Marche Apennines of central Italy. *Geology* **18**, 407–10.
- Aubourg C, Smith B, Bakhtari H, Guya N, Eshragi A, Lallemand S, Molinaro M, Braud X and Delaunay S (2004) Post-Miocene shortening pictured by magnetic fabric across the Zagros-Makran syntaxis (Iran). In *Orogenic Curvature: Integrating Paleomagnetic and Structural Analyses* (eds AJ Sussman & AB Weil), pp. 17–40. Boulder, Colorado: Geological Society of America, Special Paper 383.
- Bally AW, Burbi L, Cooper C and Ghelardoni R (1986) Balanced sections and seismic reflection profiles across the central Apennines. *Memorie della Società Geologica Italiana* **107**, 109–30.
- Barchi MR (2010) The Neogene-Quaternary evolution of the Northern Apennines: crustal structure, style of deformation and seismicity. *Journal of the Virtual Explorer* **36**, paper 11. doi: [10.3809/jvirtex.2010.00220](https://doi.org/10.3809/jvirtex.2010.00220).
- Barchi MR, Boscherini A, Collettini C, Deiana G, De Paola N, Mirabella F, Motti A and Pierantoni PP (2012) A geological map of the Colfiorito area (Umbria-Marche Apennines, Italy). Scale 1:25,000. Convegno FIST GeolItalia 01, Volume dei Riassunti, 333–4.
- Barchi MR, Minelli G and Piali G (1998) The CROP 03 profile: a synthesis of results on deep structures of the Northern Apennines. *Memorie della Società Geologica Italiana* **52**, 383–400.
- Bayona G, Thomas WA and Van der Voo R (2003) Kinematics of thrust sheets within transverse zones: a structural and paleomagnetic investigation in the Appalachian thrust belt of Georgia and Alabama. *Journal of Structural Geology* **25**, 1193–212.
- Besse J and Courtillot V (2002) Apparent and true polar wander and the geometry of the geomagnetic field over the last 200 Myr. *Journal of Geophysical Research: Solid Earth* **107**, 2300. doi: [10.1029/2000JB000050](https://doi.org/10.1029/2000JB000050).
- Billi A and Tiberti MM (2009) Possible causes of arc development in the Apennines, central Italy. *Bulletin of the Geological Society of America* **121**, 1409–20.
- Boccaletti M, Calamita F and Viandante MG (2005) The lithospheric Apennine Neo-Chain developing since the Lower Pliocene as a result of the Africa-Europe convergence. *Bollettino della Società Geologica Italiana* **124**, 87–105.
- Boccaletti M, Ciaranfi N, Cosentino D, Deiana G, Gelati R, Lentini F, Massari F, Moratti G, Pescatore T, Ricci Lucchi F and Tortorici L (1990) Palinspastic restoration and paleogeographic reconstruction of the peri-Tyrrhenian area during the Neogene. *Palaeogeography, Palaeoclimatology, Palaeoecology* **77**, 41–50.
- Calamita F (1990) Thrusts and fold-related structures in the Umbria-Marche Apennines (Central Italy). *Annales Tectonicae* **4**, 83–117.
- Calamita F, Coltorti M, Piccinini D, Pierantoni PP, Pizzi A, Ripepe M, Scisciani V and Turco E (2000) Quaternary faults and seismicity in the Umbro-Marchean Apennines (Central Italy): evidence from the 1997 Colfiorito earthquake. *Journal of Geodynamics* **29**, 245–64.
- Calamita F, Coltorti M, Pierantoni PP, Pizzi A, Scisciani V and Turco E (1997) Relazioni tra le faglie Quaternarie e la sismicità nella dorsale Appenninica umbro-marchigiana; l’area di Colfiorito. *Studi Geologici Camerti* **14**, 177–91.
- Calamita F and Deiana G (1988) The arcuate shape of the Umbria-Marche-Sabina Apennines (central Italy). *Tectonophysics* **146**, 139–47.
- Calamita F, Pace P and Satolli S (2012) Coexistence of fault-propagation and fault-bend folding in curve-shaped foreland fold-and-thrust belts: examples from the Northern Apennines (Italy). *Terra Nova* **24**, 396–406.
- Calamita F and Pierantoni PP (1993) Il sovrascorrimento di M. Cavallo - M. Primo (Appennino umbro - marchigiano). *Bollettino della Società Geologica Italiana* **112**, 825–35.

- Calamita F and Pizzi A** (1994) Recent and active extensional tectonics in the southern Umbro-Marchean Apennines (Central Italy). *Memorie della Società Geologica Italiana* **48**, 541–8.
- Calamita F, Satolli S, Scisciani V, Esestine P and Pace P** (2011) Contrasting styles of fault reactivation in curved orogenic belts: examples from the central Apennines (Italy). *Bulletin of the Geological Society of America* **123**, 1097–1111.
- Calamita F, Viandante MG and Hegarty K** (2004) Pliocene-Quaternary burial/exhumation paths of the Central Apennines (Italy); implications for the definition of the deep structure of the belt. *Bollettino della Società Geologica Italiana* **123**, 503–12.
- Carey SW** (1955) The orocline concept in geotectonics – Part I. *Papers and Proceedings of the Royal Society of Tasmania* **89**, 255–89.
- Caricchi C, Cifelli F, Sagnotti L, Sani F, Speranza F and Mattei M** (2014) Paleomagnetic evidence for a post-Eocene 90° CCW rotation of internal Apennine units: a linkage with Corsica-Sardinia rotation? *Tectonics* **33**, 374–92.
- Carmignani L and Kligfield R** (1990) Crustal extension in the northern Apennines: the transition from compression to extension in the Alpi Apuane core complex. *Tectonics* **9**, 1275–303.
- Channell JET** (1992) Paleomagnetic data from Umbria (Italy): implications for the rotation of Adria and Mesozoic apparent polar wander paths. *Tectonophysics* **216**, 365–78.
- Channell JET, Lowrie W, Medizza F and Alvarez W** (1978) Palaeomagnetism and tectonics in Umbria, Italy. *Earth and Planetary Science Letters* **39**, 199–210.
- Channell JET and McCabe C** (1994) Comparison of magnetic hysteresis parameters of unremagnetized and remagnetized limestones. *Journal of Geophysical Research* **99**, 4613–23.
- Channell JET, Oldow JS, Catalano R and D'Argenio B** (1990) Paleomagnetically determined rotations in the western Sicilian fold and thrust belt. *Tectonics* **9**, 641–60.
- Cifelli F, Caricchi C and Mattei M** (2016) Formation of arc-shaped orogenic belts in the Western and Central Mediterranean: a palaeomagnetic review. In *Palaeomagnetism in Fold and Thrust Belts: New Perspectives* (eds EL Pueyo, F Citelli, AJ Sussman & B Olivia-Urci), pp. 37–63. Geological Society of London, Special Publication no. 425.
- Cifelli F and Mattei M** (2010) Curved orogenic systems in the Italian Peninsula: a paleomagnetic review. *Journal of the Virtual Explorer* **36**, paper 17. doi: [10.3809/jvirtex.2010.00239](https://doi.org/10.3809/jvirtex.2010.00239).
- Cipollari P and Cosentino D** (1995) Miocene unconformities in the Central Apennines: geodynamic significance and sedimentary basin evolution. *Tectonophysics* **252**, 375–89.
- Cocconi R, Franchi R, Nesci O, Perilli N, Wezel FC and Battistini F** (1989) Stratigrafia, micropaleontologia e mineralogia delle Marne a Fucoidi (Aptiano inferiore-Albiano superiore) delle sezioni di Poggio le Guaine e del Fiume Bosso (Appennino Umbro-Marchigiano). In *Atti II convegno Internazionale 'Fossili, Evoluzione, Ambiente', Pergola*, pp. 163–201.
- Cogné JP** (2003) PaleoMac: a Macintosh™ application for treating paleomagnetic data and making plate reconstructions. *Geochemistry, Geophysics, Geosystems* **4**, 1007. doi: [10.1029/2001GC000227](https://doi.org/10.1029/2001GC000227).
- Coward MP, De Donatis M, Mazzoli S, Paltrinieri W and Wezel FC** (1999) Frontal part of the northern Apennines fold and thrust belt in the Romagna-Marche area (Italy): shallow and deep structural styles. *Tectonics* **18**, 559–74.
- Davis D, Suppe J and Dahlen FA** (1983) Mechanics of fold-and-thrust belts and accretionary wedges. *Journal of Geophysical Research* **88**, 1153–72.
- Deamer GA and Kodama KP** (1990) Compaction-induced inclination shallowing in synthetic and natural clay-rich sediments. *Journal of Geophysical Research* **95**, 4511–29.
- Demarest HH** (1983) Error analysis for the determination of tectonic rotation from paleomagnetic data. *Journal of Geophysical Research* **88**, 4321–8.
- Di Domenica A, Turtù A, Satolli S and Calamita F** (2012) Relationships between thrusts and normal faults in curved belts: new insight in the inversion tectonics of the Central-Northern Apennines (Italy). *Journal of Structural Geology* **42**, 104–17.
- Dogliani C** (1991) A proposal for the kinematic modelling of W-dipping subductions – possible applications to the Tyrrhenian-Apennines system. *Terra Nova* **3**, 423–34.
- Eldredge S, Bachtadse V and Van Der Voo R** (1985) Paleomagnetism and the orocline hypothesis. *Tectonophysics* **119**, 153–79.
- Enkin RJ and Watson GS** (1996) Statistical analysis of palaeomagnetic inclination data. *Geophysical Journal International* **126**, 781–95.
- Faccenna C, Davy P, Brun JP, Funicello R, Giardini D, Mattei M and Nalpas T** (1996) The dynamics of back-arc extension: an experimental approach to the opening of the Tyrrhenian Sea. *Geophysical Journal International* **126**, 781–95.
- Faccenna C, Piromallo C, Crespo-Blanc A, Jolivet L and Rossetti F** (2004) Lateral slab deformation and the origin of the western Mediterranean arcs. *Tectonics* **23**, TC1012. doi: [10.1029/2002TC001488](https://doi.org/10.1029/2002TC001488).
- Finetti IR** (2005) CROP PROJECT: Deep Seismic Exploration of the Central Mediterranean and Italy. Amsterdam: Elsevier, 794 pp.
- Fisher R** (1953) Dispersion on a sphere. *Proceedings of the Royal Society A: Mathematical, Physical and Engineering Sciences* **217**, 195–305.
- Fossen H** (2010) *Structural Geology*. Cambridge: Cambridge University Press, 463 pp.
- Gattacceca J and Speranza F** (2002) Paleomagnetism of Jurassic to Miocene sediments from the Apenninic carbonate platform (southern Apennines, Italy): evidence for a 60° counterclockwise Miocene rotation. *Earth and Planetary Science Letters* **201**, 19–34.
- Gradstein FM, Ogg JG, Schmitz MD, Ogg GM, Gradstein FM and Ali A** (2012) *The Geologic Time Scale 2012*. Amsterdam: Elsevier, 1176 pp.
- Hindle D and Burkhard M** (1999) Strain, displacement and rotation associated with the formation of curvature in fold belts; the example of the Jura arc. *Journal of Structural Geology* **21**, 1089–101.
- Jackson KC** (1990) A palaeomagnetic study of Apennine thrusts, Italy: Monte Maiella and Monte Raparo. *Tectonophysics* **178**, 231–40.
- Johnston ST and Mazzoli S** (2009) The Calabrian Orocline: buckling of a previously more linear orogen. In *Ancient Orogens and Modern Analogues* (eds JB Murphy, JD Keppie & AJ Hynes), pp. 113–25. Geological Society of London, Special Publication no. 327.
- Jolivet L, Dubois R, Fournier M, Goffe B, Michard A and Jourdan C** (1990) Ductile extension in alpine Corsica. *Geology* **18**, 1007–10.
- Kirschvink JL** (1980) The least-squares line and plane and the analysis of palaeomagnetic data. *Geophysical Journal of the Royal Astronomical Society* **62**, 699–718.
- Koymans MR, Langereis CG, Pastor-Galán D and van Hinsbergen DJJ** (2016) Paleomagnetism.org: an online multi-platform open source environment for paleomagnetic data analysis. *Computers and Geosciences* **93**, 127–37.
- Kwon S and Mitra G** (2004) Strain distribution, strain history, and kinematic evolution associated with the formation of arcuate salients in fold-thrust belts; the example of the Provo salient, Sevier orogen, Utah. In *Orogenic Curvature – Integrating Paleomagnetic and Structural Analyses* (eds AJ Sussman & AB Weil), pp. 205–23. Boulder, Colorado: Geological Society of America, Special Paper 383.
- Lacombe O, Mouthereau F, Angelier J, Chu HT and Lee JC** (2003) Frontal belt curvature and oblique ramp development at an obliquely collided irregular margin: geometry and kinematics of the NW Taiwan fold-thrust belt. *Tectonics* **22**, 1–16.
- Lacquement F, Averbuch O, Mansy JL, Szaniawski R and Lewandowski M** (2005) Transpressional deformations at lateral boundaries of propagating thrust-sheets: the example of the Meuse Valley Recess within the Ardennes Variscan fold-and-thrust belt (N France-S Belgium). *Journal of Structural Geology* **27**, 1788–802.
- Lavecchia G** (1985) Il sovrascorrimento dei Monti Sibillini: analisi cinematica e strutturale. *Bollettino della Società Geologica Italiana* **104**, 161–94.
- Lickorish WH, Ford M, Bürgisser J and Cobbold PR** (2002) Arcuate thrust systems in sandbox experiments: a comparison to the external arcs of the Western Alps. *Bulletin of the Geological Society of America* **114**, 1089–107.
- Lu G, Marshak S and Kent DV** (1990) Characteristics of magnetic carriers responsible for Late Paleozoic remagnetization in carbonate strata of the mid-continent, U.S.A. *Earth and Planetary Science Letters* **102**, 351–61.
- Lucente FP and Speranza F** (2001) Belt bending driven by lateral bending of subducting lithospheric slab: geophysical evidences from the Northern Apennines (Italy). *Tectonophysics* **337**, 53–64.

- Macedo J and Marshak S** (1999) Controls on the geometry of fold-thrust belt salients. *Bulletin of the Geological Society of America* **111**, 1808–22.
- Malinverno A and Ryan WBF** (1986) Extension in the Tyrrhenian Sea and shortening in the Apennines as result of arc migration driven by sinking of the lithosphere. *Tectonics* **5**, 227–45.
- Marshak S** (1988) Kinematics of orocline and arc formation in thin-skinned orogens. *Tectonics* **7**, 73–86.
- Marshak S** (2004) Salients, recesses, arcs, oroclines, and syntaxes – a review of ideas concerning the formation of map-view curves in fold-thrust belts. *AAPG Memoir* **82**, 131–56.
- Marshak S, Wilkerson MS and Hsui AT** (1992) Generation of curved fold-thrust belts: insight from simple physical and analytical models. In *Thrust Tectonics*, pp. 83–92. London: Chapman & Hall.
- Martori P and D'Andrea M** (1992) Paleomagnetically inferred rotations of the Abruzzi and Northwestern Umbria. *Tectonophysics* **202**, 43–53.
- Mattei M, Funicello R and Kissel C** (1995) Paleomagnetic and structural evidence for Neogene block rotations in the Central Apennines, Italy. *Journal of Geophysical Research* **100**, 863–83.
- Mattei M, Kissel C and Funicello R** (1996) No tectonic rotation of the Tuscan Tyrrhenian margin (Italy) since Late Messinian. *Journal of Geophysical Research* **101**, 2835–45.
- McFadden PL** (1990) A new fold test for palaeomagnetic studies. *Geophysical Journal International* **103**, 163–9.
- McFadden PL and McElhinny MW** (1988) The combined analysis of remagnetization circles and direct observations in palaeomagnetism. *Earth and Planetary Science Letters* **87**, 161–72.
- McFadden PL and McElhinny MW** (1990) Classification of the reversal test in palaeomagnetism. *Geophysical Journal International* **103**, 725–9.
- Muttoni G, Argnani A, Kent DV, Abrahamsen N and Cibin U** (1998) Paleomagnetic evidence for Neogene tectonic rotations in the northern Apennines, Italy. *Earth and Planetary Science Letters* **154**, 25–40.
- Muttoni G, Garzanti E, Alfonsi L, Cirilli S, Germani D and Lowrie W** (2001) Motion of Africa and Adria since the Permian: paleomagnetic and paleoclimatic constraints from northern Libya. *Earth and Planetary Science Letters* **192**, 159–74.
- Pace P and Calamita F** (2014) Push-up inversion structures v. Fault-bend reactivation anticlines along oblique thrust ramps: examples from the Apennines fold-and-thrust belt (Italy). *Journal of the Geological Society* **171**, 227–38.
- Pace P and Calamita F** (2015) Coalescence of fault-bend and fault-propagation folding in curved thrust systems: an insight from the Central Apennines, Italy. *Terra Nova* **27**, 175–83.
- Pace P, Pasqui V, Tavarnelli E and Calamita F** (2017) Foreland-directed gravitational collapse along curved thrust fronts: insights from a minor thrust-related shear zone in the Umbria-Marche belt, central-northern Italy. *Geological Magazine* **154**, 381–92.
- Pastor-Galán D, Gutiérrez-Alonso G, Mulchrone KF and Huerta P** (2012) Conical folding in the core of an orocline. A geometric analysis from the Cantabrian Arc (Variscan Belt of NW Iberia). *Journal of Structural Geology* **39**, 210–23.
- Pastor-Galán D, Mulchrone KF, Koymans MR, van Hinsbergen DJJ and Langereis CG** (2017) Bootstrapped total least squares orocline test: a robust method to quantify vertical-axis rotation patterns in orogens, with examples from the Cantabrian and Aegean oroclines. *Lithosphere* **9**, 499–511.
- Pueyo EL, Pocoví A., Parés JM, Millán H and Larrasoana JC** (2003) Thrust ramp geometry and spurious rotations of paleomagnetic vectors. *Studia Geophysica et Geodaetica* **47**, 331–57.
- Pueyo EL, Sussman AJ, Oliva-Urcia B and Cifelli F** (2016) Palaeomagnetism in fold and thrust belts: use with caution. In *Palaeomagnetism in Fold and Thrust Belts: New Perspectives* (eds EL Pueyo, F Cifelli, AJ Sussman & B Oliva-Urci), pp. 259–76. Geological Society of London, Special Publication no. 425.
- Rodríguez-Pintó A., Pueyo EL, Calvin P, Sánchez E, Ramajo J, Casas AM, Ramón MJ, Pocoví A, Barnolas A and Román T** (2016) Rotational kinematics of a curved fold: the Balzes anticline (Southern Pyrenees). *Tectonophysics* **677–678**, 171–89.
- Santantonio M** (1993) Facies associations and evolution of pelagic carbonate platform/basin systems: examples from the Italian Jurassic. *Sedimentology* **40**, 1039–67.
- Satolli S, Besse J and Calamita F** (2008) Paleomagnetism of Aptian-Albian sections from the Northern Apennines (Italy): implications for the 150–100 Ma apparent polar wander of Adria and Africa. *Earth and Planetary Science Letters* **276**, 115–28.
- Satolli S, Besse J, Speranza F and Calamita F** (2007) The 125–150 Ma high-resolution Apparent Polar Wander Path for Adria from magnetostratigraphic sections in Umbria-Marche (Northern Apennines, Italy): timing and duration of the global Jurassic-Cretaceous hairpin turn. *Earth and Planetary Science Letters* **257**, 329–42.
- Satolli S and Calamita F** (2008) Differences and similarities between the central and the southern Apennines (Italy): examining the Gran Sasso versus the Matese-Frosolone salients using paleomagnetic, geological, and structural data. *Journal of Geophysical Research: Solid Earth* **113**, B10101. doi: [10.1029/2011JB008292](https://doi.org/10.1029/2011JB008292).
- Satolli S and Calamita F** (2012) Influence of inversion tectonics in the bending of a foreland fold-and-thrust belt: the case of the northern Apennines (Italy). *Journal of the Virtual Explorer* **43**, paper 5. [10.3809/jvirtex.2012.00302](https://doi.org/10.3809/jvirtex.2012.00302).
- Satolli S, Speranza F and Calamita F** (2005) Paleomagnetism of the Gran Sasso range salient (central Apennines, Italy): pattern of orogenic rotations due to translation of a massive carbonate indenter. *Tectonics* **24**, TC4019. doi: [10.1029/2004TC001771](https://doi.org/10.1029/2004TC001771).
- Satolli S and Turtù A** (2016) Early Cretaceous magnetostratigraphy of the Salto del Cieco section (Northern Apennines, Italy). *Newsletters on Stratigraphy* **49**, 361–82.
- Scheepers PJJ and Langereis CG** (1994) Paleomagnetic evidence for counter-clockwise rotations in the Southern Apennines fold-and-thrust belt during the late Pliocene and middle Pleistocene. *Tectonophysics* **239**, 43–59.
- Scisciani V, Agostini S, Calamita F, Pace P, Cilli A, Giori I and Paltrinieri W** (2014) Positive inversion tectonics in foreland fold-and-thrust belts: a reappraisal of the Umbria-Marche Northern Apennines (Central Italy) by integrating geological and geophysical data. *Tectonophysics* **637**, 218–37.
- Scisciani V and Montefalcone R** (2006) Coexistence of thin- and thick-skinned tectonics: an example from the Central Apennines, Italy. In *Styles of Continental Contraction* (eds S Mazzoli & RWH Butler), pp. 33–54. Boulder, Colorado: Geological Society of America, Special Papers 414.
- Scisciani V, Rusciadelli G and Calamita F** (2000) Faglie normali nell'evoluzione tortoniano-messiniana dei bacini sinorogenici dell'Appennino centrale esterno. *Bollettino della Società Geologica Italiana* **119**, 715–32.
- Scisciani V, Tavarnelli E, Calamita F and Paltrinieri W** (2002) Pre-thrusting normal faults within syn-orogenic basins of the Outer Central Apennines, Italy: implications for Apennine tectonics. *Bollettino della Società Geologica Italiana* **1**, 295–304.
- Smith B, Aubourg C, Guézou JC, Nazari H, Molinaro M, Braud X and Guya N** (2005) Kinematics of a sigmoidal fold and vertical axis rotation in the east of the Zagros-Makran syntaxis (southern Iran): paleomagnetic, magnetic fabric and microtectonic approaches. *Tectonophysics* **411**, 89–109.
- Speranza F, Maniscalco R and Grasso M** (2003) Pattern of orogenic rotations in central-eastern Sicily: implications for the timing of spreading in the Tyrrhenian Sea. *Journal of the Geological Society, London* **160**, 183–95.
- Speranza F, Mattei M, Naso G, Di Bucci D and Corrado S** (1998) Neogene-Quaternary evolution of the central Apennine orogenic system (Italy): a structural and palaeomagnetic approach in the Molise region. *Tectonophysics* **299**, 143–57.
- Speranza F, Sagnotti L and Mattei M** (1997) Tectonics of the Umbria-Marche-Romagna Arc (central northern Apennines, Italy): new paleomagnetic constraints. *Journal of Geophysical Research B: Solid Earth* **102**, 3153–66.
- Tarduno JA, Lowrie W, Sliter WV, Bralower TJ and Heller F** (1992) Reversed polarity characteristic magnetizations in the Albian Contessa section, Umbrian Apennines, Italy: implications for the existence of a mid-Cretaceous mixed polarity interval. *Journal of Geophysical Research* **97**, 241–71.
- Tavarnelli E** (1993) Evidence for fault propagation folding in the Umbria-Marche-Sabina Apennines (Central Italy). *Annales Tectonicae* **7**, 87–99.
- Tavarnelli E** (1997) Structural evolution of a foreland fold-and-thrust belt: the Umbria-Marche Apennines, Italy. *Journal of Structural Geology* **19**, 523–34.
- Tavarnelli E, Butler RWH, Decandia FA, Calamita F, Alvarez W and Renda P** (2004) Implications of fault reactivation and structural inheritance in the Cenozoic tectonic evolution of Italy. In *The Geology of Italy*

- (eds U Crescenti, S. D'Offizi, S Merlino & L Sacchi), pp. 209–22. Florence: Italian Geological Society.
- Thébaud E, Finlay CC, Beggan CD, Alken P, Aubert J, Barrois O, Bertrand F, Bondar T, Boness A, Brocco L, Canet E, Chambodut A, Chulliat A, Coïsson P, Civet F, Du A, Fournier A, Fratter I, Gillet N, Hamilton B, Hamoudi M, Hulot G, Jager T, Korte M, Kuang W, Lalanne X, Langlais B, Léger JM, Lesur V, Lowes FJ, Macmillan S, Manda M, Manoj C, Maus S, Olsen N, Petrov V, Ridley V, Rother M, Sabaka TJ, Saturnino D, Schachtschneider R, Sirol O, Tangborn A, Thomson A, Toffner-Clausen L, Vigneron P, Wardinski I and Zvereva T** (2015) International geomagnetic reference field: the 12th generation. *Earth, Planets and Space* **67**, 79. doi: [10.1186/s40623-015-0228-9](https://doi.org/10.1186/s40623-015-0228-9).
- Tozer RSJ, Butler RWH and Corrado S** (2002) Comparing thin- and thick-skinned thrust tectonic models of the Central Apennines, Italy. *Stephan Mueller Special Publication Series* **1**, 181–94.
- Turtù A., Satolli S, Maniscalco R, Calamita F and Speranza F** (2013) Understanding progressive-arc- and strike-slip-related rotations in curve-shaped orogenic belts: the case of the Olevano-Antrodoco-Sibillini thrust (Northern Apennines, Italy). *Journal of Geophysical Research: Solid Earth* **118**, 459–73.
- Van der Voo R** (1990) The reliability of paleomagnetic data. *Tectonophysics* **184**, 1–9.
- Van der Voo R** (1993) *Paleomagnetism of the Atlantic, Tethys and Iapetus Oceans*. Cambridge: Cambridge University Press, 411 pp.
- Weil AB and Sussman AJ** (2004) Classifying curved orogens based on timing relationships between structural development and vertical-axis rotations. In *Orogenic Curvature: Integrating Paleomagnetic and Structural Analyses* (eds AJ Sussman & AB Weil), pp. 1–15. Boulder, Colorado: Geological Society of America, Special Paper 383.
- Weil AB, Yonkee A and Sussman A** (2010) Reconstructing the kinematic evolution of curved mountain belts: a paleomagnetic study of Triassic red beds from the Wyoming salient, Sevier thrust belt, U.S.A. *Bulletin of the Geological Society of America* **122**, 24–49.
- Zijderveld JDA** (1967) A.C. demagnetization of rocks: analysis of results. In *Methods in Palaeomagnetism* (eds DW Collinson, KM Creer & SK Runcorn), pp. 254–86. Amsterdam: Elsevier.